10. Konstam MA, Neaton JD, Dickstein K, Drexler H, Komajda M, Martinez FA, Riegger GA, Malbecq W, Smith RD, Guptha S, Poole-Wilson PA. Effects of high-dose versus low-dose losartan on clinical outcomes in patients with heart failure (HEAAL study): a randomised, double-blind trial. *Lancet* 2009;**374**:1840–1848.
11. Radford MJ, Arnold JM, Bennett SJ, Cinquegrani MP, Cleland JG, Havranek EP, Heidenreich PA, Rutherford JD, Spertus JA, Stevenson LW, Goff DC, Grover FL, Malenka DJ, Peterson ED, Redberg RF. ACC/AHA key data elements and definitions for measuring the clinical management and outcomes of patients with chronic heart failure: a report of the American College of Cardiology/American Heart Association Task Force on Clinical Data Standards (Writing Committee to Develop Heart Failure Clinical Data Standards): developed in collaboration with the American College of Chest Physicians and the International Society for Heart and Lung Transplantation: endorsed by the Heart Failure Society of America. *Circulation* 2005;**112**:1888–1916.
12. Hall MJ, Levant S, DeFrances CJ. Hospitalization for congestive heart failure: United States. *NCHS Data Brief* 2000–2010;**2012**:1–8.
13. Mortara A, La Rovere MT, Pinna GD, Prpa A, Maestri R, Febo O, Pozzoli M, Opasich C, Tavazzi L. Arterial baroreflex modulation of heart rate in chronic heart failure: clinical and hemodynamic correlates and prognostic implications. *Circulation* 1997;**96**:3450–3458.
14. La Rovere MT, Bigger JT Jr, Marcus FI, Mortara A, Schwartz PJ. Baroreflex sensitivity and heart-rate variability in prediction of total cardiac mortality after myocardial infarction. ATRAMI (Autonomic Tone and Reflexes After Myocardial Infarction) Investigators. *Lancet* 1998;**351**:478–484.
15. Li M, Zheng C, Sato T, Kawada T, Sugimachi M, Sunagawa K. Vagal nerve stimulation markedly improves long-term survival after chronic heart failure in rats. *Circulation* 2004;**109**:120–124.
16. Li M, Zheng C, Inagaki M, Kawada T, Sunagawa K, Sugimachi M. Chronic vagal stimulation decreased vasopressin secretion and sodium ingestion in heart failure rats after myocardial infarction. *Conf Proc IEEE Eng Med Biol Soc* 2005;**4**:3962–3965.
17. De Ferrari GM, Crijns HJ, Borggrefe M, Milasinovic G, Smid J, Zabel M, Gavazzi A, Sanzo A, Dennert R, Kuschyk J, Raspopovic S, Klein H, Swedberg K, Schwartz PJ. Chronic vagus nerve stimulation: a new and promising therapeutic approach for chronic heart failure. *Eur Heart J* 2011;**32**:847–855.
18. Schwartz PJ. Vagal stimulation for heart diseases: from animals to men. An example of translational cardiology. *Neth Heart J* 2013;**21**:82–84.
19. Lazartigues E, Freslon JL, Tellioglu T, Brefel-Courbon C, Pelat M, Tran MA, Montastruc JL, Rascol O. Pressor and bradycardic effects of tacrine and other acetylcholinesterase inhibitors in the rat. *Eur J Pharmacol* 1998;**361**:61–71.
20. Androne AS, Hryniewicz K, Goldsmith R, Arwady A, Katz SD. Acetylcholinesterase inhibition with pyridostigmine improves heart rate recovery after maximal exercise in patients with chronic heart failure. *Heart* 2003;**89**:854–858.
21. Okazaki Y, Zheng C, Li M, Sugimachi M. Effect of the cholinesterase inhibitor donepezil on cardiac remodeling and autonomic balance in rats with heart failure. *J Physiol Sci* 2010;**60**:67–74.
22. Li M, Zheng C, Kawada T, Inagaki M, Uemura K, Shishido T, Sugimachi M. Donepezil markedly improves long-term survival in rats with chronic heart failure after extensive myocardial infarction. *Circ J* 2013;**77**:2519–2525.
23. Lefebvre F, Préfontaine A, Calderone A, Caron A, Jasmin JF, Villeneuve L, Dupuis J. Modification of the pulmonary renin-angiotensin system and lung structural remodelling in congestive heart failure. *Clin Sci (Lond)* 2006;**111**:217–224.
24. Kawada T, Li M, Kamiya A, Shimizu S, Uemura K, Yamamoto H, Sugimachi M. Open-loop dynamic and static characteristics of the carotid sinus baroreflex in rats with chronic heart failure after myocardial infarction. *J Physiol Sci* 2010;**60**:283–298.
25. Suga H. *Ventricular energetics. Physiol Rev* 1990;**70**:247–277.
26. Bristow MR. Treatment of chronic heart failure with β-adrenergic receptor antagonists: a convergence of receptor pharmacology and clinical cardiology. *Circ Res* 2011;**109**:1176–1194.
27. Swedberg K1, Komajda M, Böhm M, Borer JS, Ford I, Dubost-Brama A, Lerebours G, Tavazzi L, SHIFT Investigators, Ivabradine and outcomes in chronic heart failure (SHIFT): a randomised placebo-controlled study. *Lancet* 2010;**376**: 875–85.
28. Matsuura W, Sugimachi M, Kawada T, Sato T, Shishido T, Miyano H, Nakahara T, Ikeda Y, Alexander J Jr, Snagawa K. Vagal stimulation decreases left ventricular contractility mainly through negative chronotropic effect. *Am J Physiol* 1997;**273**:H534–H539.
29. Nakayama Y, Miyano H, Shishido T, Inagaki M, Kawada T, Sugimachi M, Sunagawa K. Heart rate-independent vagal effect on end-systolic elastance of the canine left ventricle under various levels of sympathetic tone. *Circulation* 2001;**104**:2277–2279.
30. Joaquim LF, Farah VM, Bernatova I, Fazan R Jr, Grubbs R, Morris M. Enhanced heart rate variability and baroreflex index after stress and cholinesterase inhibition in mice. *Am J Physiol Heart Circ Physiol* 2004;**287**:H251–H257.
31. Singer W, Opfer-Gehrking TL, Nickander KK, Hines SM, Low PA. Acetylcholinesterase inhibition in patients with orthostatic intolerance. *J Clin Neurophysiol* 2006;**23**:476–481.
32. Rosas-Ballina M, Tracey KJ. Cholinergic control of inflammation. *J Intern Med* 2009;**265**:663–679.
33. Mann DL. Inflammatory mediators and the failing heart: past, present, and the foreseeable future. *Circ Res* 2002;**91**:988–998.
34. Springer J, Okonko DO, Anker SD. Vagal nerve stimulation in chronic heart failure: an antiinflammatory intervention? *Circulation 2004*;**110**:e34; author reply e34.
35. Schellings MW, Pinto YM, Heymans S. Matricellular proteins in the heart: possible role during stress and remodeling. *Cardiovasc Res* 2004;**64**:24–31.
36. Ertl G, Frantz S. Healing after myocardial infarction. *Cardiovasc Res* 2005;**66**:22–32.
37. Heeschen C, Weis M, Aicher A, Dimmeler S, Cooke JP. A novel angiogenic pathway mediated by non-neuronal nicotinic acetylcholine receptors. *J Clin Invest* 2002;**110**:527–536.
38. Zheng W, Brown MD, Brock TA, Bjercke RJ, Tomanek RJ. Bradycardia-induced coronary angiogenesis is dependent on vascular endothelial growth factor. *Circ Res* 1999;**85**:192–198.
39. Milavetz JJ, Raya TE, Johnson CS, Morkin E, Goldman S. Survival after myocardial infarction in rats: captopril versus losartan. *J Am Coll Cardiol* 1996;**27**:714–719.
40. Cohn JN, Tognoni G, Valsartan Heart Failure Trial Investigators. A randomized trial of the angiotensin-receptor blocker valsartan in chronic heart failure. *N Engl J Med* 2001;**345**:1667–1675.
41. Richer C, Fornes P, Cazaubon C, Domergue V, Nisato D, Giudicelli JF. Effects of long-term angiotensin II AT1 receptor blockade on survival, hemodynamics and cardiac remodeling in chronic heart failure in rats. *Cardiovasc Res* 1999;**41**:100–108.
42. Takahashi M, Tanonaka K, Yoshida H, Oikawa R, Koshimizu M, Daicho T, Toyo-Oka T, Takeo S. Effects of ACE inhibitor and AT1 blocker on dystrophin-related proteins and calpain in failing heart. *Cardiovasc Res* 2005;**65**:356–365.
43. Urata H, Kinoshita A, Misono KS, Bumpus FM, Husain A. Identification of a highly specific chymase as the major angiotensin II-forming enzyme in the human heart. *J Biol Chem* 1990;**265**:22348–22357.
44. Lanctôt PM, Leclerc PC, Escher E, Leduc R, Guillemette G. Role of N-glycosylation in the expression and functional properties of human AT1 receptor. *Biochemistry* 1999;**38**:8621–8627.
45. Pfeffer MA, Pfeffer JM, Steinberg C, Finn P. Survival after an experimental myocardial infarction: beneficial effects of long-term therapy with captopril. *Circulation* 1985;**72**:406–412.
46. Ahmet I, Morrell C, Lakatta EG, Talan MI. Therapeutic efficacy of a combination of a beta1-adrenoreceptor (AR) blocker and beta2-AR agonist in a rat model of postmyocardial infarction dilated heart failure exceeds that of a beta1-AR blocker plus angiotensin-converting enzyme inhibitor. *J Pharmacol Exp Ther* 2009;**331**:178–185.
47. White HD, Aylward PE, Huang Z, Dalby AJ, Weaver WD, Barvik S, Marin-Neto JA, Murin J, Nordlander RO, van Gilst WH, Zannad F, McMurray JJ, Califf RM, Pfeffer MA. Mortality and morbidity remain high despite captopril and/or valsartan therapy in elderly patients with left ventricular systolic dysfunction, heart failure, or both after acute myocardial infarction: results from the Valsartan in Acute Myocardial Infarction Trial (VALIANT). *Circulation* 2005;**112**:3391–3399.
48. Nordström P, Religa D, Wimo A, Winblad B, Eriksdotter M. The use of cholinesterase inhibitors and the risk of myocardial infarction and death: a nationwide cohort study in subjects with Alzheimer's disease. *Eur Heart J* 2013;**34**:2585–2591.

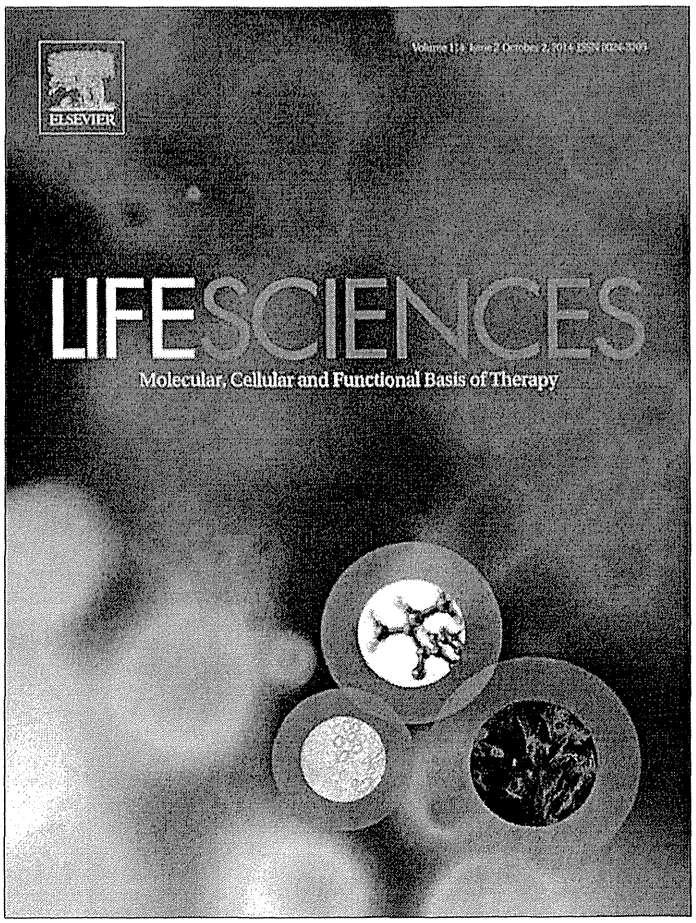

Life Sciences 114 (2014) 102–106

Contents lists available at ScienceDirect

Life Sciences

journal homepage: www.elsevier.com/locate/lifescie

Effects of intravenous cariporide on release of norepinephrine and myoglobin during myocardial ischemia/reperfusion in rabbits

Shigeru Sakurai [a], Yosuke Kuroko [a], Shuji Shimizu [a,b,*], Toru Kawada [b], Tsuyoshi Akiyama [c], Toji Yamazaki [d], Masaru Sugimachi [b], Shunji Sano [a]

[a] Department of Cardiovascular Surgery, Okayama University Graduate School of Medicine, Dentistry and Pharmaceutical Sciences, Okayama 700-8558, Japan
[b] Department of Cardiovascular Dynamics, National Cerebral and Cardiovascular Center, Osaka 565-8565, Japan
[c] Department of Cardiac Physiology, National Cerebral and Cardiovascular Center, Osaka 565-8565, Japan
[d] Department of Anesthesiology, National Hospital Organization Kinki-Chuo Chest Medical Center, Osaka 591-8555, Japan

ARTICLE INFO

Article history:
Received 12 May 2014
Accepted 8 August 2014
Available online 17 August 2014

Keywords:
Cariporide
Myoglobin
Norepinephrine
Ischemia/reperfusion

ABSTRACT

Aims: To examine the effects of cariporide, a Na^+/H^+ exchanger-1 inhibitor, on cardiac norepinephrine (NE) and myoglobin release during myocardial ischemia/reperfusion by applying a microdialysis technique to the rabbit heart.

Main methods: In anesthetized rabbits, two dialysis probes were implanted into the left ventricular myocardium and were perfused with Ringer's solution. Cariporide (0.3 mg/kg) was injected intravenously, followed by occlusion of the left circumflex coronary artery. During 30-min coronary occlusion followed by 30-min reperfusion, four consecutive 15-min dialysate samples (two during ischemia and two during reperfusion) were collected in vehicle and cariporide-treated groups. Dialysate myoglobin and NE concentrations were measured by immunochemistry and high-performance liquid chromatography, respectively.

Key findings: Dialysate myoglobin and NE concentrations increased significantly during myocardial ischemia/reperfusion in both vehicle and cariporide-treated groups ($P < 0.01$ vs. baseline). In cariporide-treated group, dialysate myoglobin concentrations were significantly lower than those in vehicle group throughout ischemia/reperfusion ($P < 0.01$ at 0–15 min of ischemia, $P < 0.05$ at 15–30 min of ischemia, $P < 0.01$ at 0–15 min of reperfusion, and $P < 0.01$ at 15–30 min of reperfusion). However, dialysate NE concentrations in cariporide-treated group were lower than those in vehicle group only during ischemia ($P < 0.01$ at 0–15 min of ischemia, and $P < 0.05$ at 15–30 min of ischemia).

Significance: When administered before ischemia, cariporide reduces myoglobin release during ischemia/reperfusion and decreases NE release during ischemia.

Introduction

The Na^+/H^+ exchanger isoform-1 (NHE-1) is a ubiquitously expressed integral membrane protein transporter that regulates intracellular pH by removing intracellular H^+ in exchange for extracellular Na^+ (Fliegel, 2005). NHE-1 has been reported to play an important role in the pathogenesis of myocardial ischemia/reperfusion injuries (Avkiran, 1999, 2003). During myocardial ischemia/reperfusion, the activity or quantity of NHE-1 increases, leading to an accumulation of intracellular Na^+, which in turn reduces and eventually reverses the driving force for the Na^+/Ca^{2+} exchanger, thereby decreasing Ca^{2+} efflux and eventually increasing Ca^{2+} influx. This process subsequently induces intracellular Ca^{2+} overload and promotes structural (apoptosis) and functional (arrhythmias, hypercontraction) damages (Leineweber et al., 2007). In sympathetic nerve endings, increased NHE-1 activity results in accumulation of axoplasmic Na^+ that diminishes the inward transport and eventually favors the outward transport of norepinephrine (NE) via the neuronal NE transporter (a bidirectional NE carrier, NET) (Leineweber et al., 2007). Thus, inhibition of NHE-1 may reduce NE release into the synaptic cleft. Because excessive NE release from sympathetic nerve endings is a prominent cause of arrhythmias and cardiac dysfunction (Leineweber et al., 2007), NHE-1 inhibitors may provide cardioprotection against functional damage during ischemia/reperfusion.

Cariporide, a NHE-1 inhibitor, has been reported to be a pharmacologically preconditioning agent. Several experimental studies have demonstrated that pretreatment with cariporide reduces infarct size (Kristo et al., 2004; Miura et al., 1997), suggesting that the inhibition of NHE-1 protects the heart from structural damage during ischemia/reperfusion. Furthermore, Létienne et al. (2006) reported that cariporide significantly reduced plasma myoglobin and troponin I

* Corresponding author at: Department of Cardiovascular Dynamics, National Cerebral and Cardiovascular Center, 5-7-1 Fujishiro-dai, Suita, Osaka 565-8565, Japan. Tel.: +81 6 6833 5012; fax: +81 6 6835 5403.
E-mail address: shujismz@ri.ncvc.go.jp (S. Shimizu).

http://dx.doi.org/10.1016/j.lfs.2014.08.008
0024-3205/

levels that strongly correlated with myocardial necrosis. Therefore, cariporide treatment before ischemia may reduce both pathological NE release and structural damage of the heart during ischemia/reperfusion. However, because of the limited methodology for simultaneous monitoring NE release and structural heart damage in the past, the mechanism of cardioprotection by cariporide has not been fully elucidated. Our group has already demonstrated that cardiac microdialysis technique can simultaneously monitor interstitial NE and myoglobin levels in the ischemic region of the left ventricle (Kitagawa et al., 2005). Because there is less blood flow in ischemic lesion, diffusion of myoglobin should be limited. Therefore interstitial myoglobin level monitored by cardiac microdialysis technique may serve as a more accurate index of structural damage of the heart than plasma myoglobin level. Using this technique, we investigated the effects of cariporide on both NE and myoglobin releases in the left ventricle during ischemia/reperfusion.

Materials and methods

Animal preparation

Animal care was provided in accordance with the *Guiding Principles for the Care and Use of Animals in the Field of Physiological Sciences* approved by the Physiological Society of Japan. All protocols were approved by the Animal Subject Committee of the National Cerebral and Cardiovascular Center. Twelve adult male Japanese white rabbits weighing from 2.5 to 3.5 kg were anesthetized with an intravenous injection of pentobarbital sodium (40 mg/kg) via the marginal ear vein, followed by continuous intravenous infusion of pentobarbital sodium (2 mg/kg/h). Butorphanol (0.1 mg/kg) was injected intramuscularly every 2–3 h for analgesia. Adequate anesthesia level was confirmed by loss of the ear pinch response. The rabbits were intubated and ventilated mechanically with room air mixed with oxygen. Systemic arterial pressure was monitored by a catheter inserted into the femoral artery. Heparin sodium (10 IU/kg/h) was infused to prevent blood coagulation in the femoral artery catheter. Heart rate was monitored on body surface electrocardiogram. Arterial pressure and heart rate were recorded by a PowerLab Data Acquisition System (ADInstruments, Dunedin, New Zealand). Esophageal temperature was maintained between 38 and 39 °C using a heating pad.

With the animal in the lateral position, the fifth or sixth rib on the left side was partially removed and a small incision was made in the pericardium to expose the heart. A snare was placed around the main branch of the left circumflex coronary artery (LCX) to act as an occluder for later coronary occlusion. Two dialysis probes were implanted in the left ventricular wall corresponding to the region perfused by the LCX. To confirm that the dialysis probes were properly located inside the ischemic region, we examined the color and motion of the ventricular wall during a brief occlusion. To avoid a preconditioning effect, the duration of brief occlusion was limited to a few seconds.

At the end of each experiment, the LCX was again occluded. Evans blue (1%) was intravenously injected to confirm that the dialysis probes were properly implanted within the ischemic area. The rabbits were euthanized by injecting an overdose of pentobarbital sodium. At postmortem, the heart was excised from the euthanized rabbit and was transversely sliced into 3 or 4 pieces. The left ventricular cavity was macroscopically examined to confirm that the dialysis membranes were not exposed to the left ventricular cavity.

Dialysis technique

Materials for cardiac microdialysis probe have been described in detail previously (Akiyama et al., 1991; Kitagawa et al., 2005). The long transverse dialysis probes were custom made. For monitoring myocardial interstitial NE levels, a dialysis fiber (length 8 mm, o.d. 0.31 mm, i.d. 0.20 mm; PAN-1200 50,000 molecular weight cutoff; Asahi Chemical Japan) was glued at both ends to polyethylene tubes. This dialysis probe was perfused with Ringer's solution at a rate of 2 μl/min using a microinjection pump (Carnegie Medicine CMA/102, Sweden). Each dialysate sample was collected over 15 min (1 sampling volume = 30 μl) into a microtube containing 3 μl of 0.1 N HCl to prevent amine oxidation. Dialysate NE level was measured by high-performance liquid chromatography with electrochemical detection (ECD-300, Eicom, Japan) as described in the Analytical procedures section.

For monitoring myocardial interstitial myoglobin levels, another dialysis probe (length 8 mm, o.d. 0.215 mm, i.d. 0.175 mm, 300 Å pore size; Evaflux type 5A; Kuraray Medical, Japan) was used as described previously (Kitagawa et al., 2005). This dialysis probe was perfused with Ringer's solution at a rate of 5 μl/min. Dialysate sampling period was 15 min (1 sampling volume = 75 μl). Dialysate myoglobin concentration was measured by immunochemistry using a Cardiac Reader (Roche Diagnostics, Basel, Switzerland) as described in the Analytical procedures section.

Experimental protocols were started 2 h after implantation of the dialysis probes. During dialysate sampling, we took into account the dead space between the dialysis membrane and the sample tube.

Analytical procedures

Dialysate NE concentrations were measured by high-performance liquid chromatography with electrochemical detection. An alumina procedure was employed to remove the interfering compounds from the dialysate samples. The liquid chromatography system consisted of a pump (EP-300, Eicom) with a degasser (DG-300, Eicom), a separation column (Eicompak CA-5ODS, Eicom), and an electrochemical detector (ECD-300, Eicom). The temperature of the separation was maintained at 25 °C by a column oven (ATC-300, Eicom). The electrochemical detector was operated with a graphite electrode (WE-3G, Eicom) at +0.45 V vs. an Ag/AgCl reference electrode. Mobile phase consisted of 12% (v/v) methanol, 1-octanesulfonic acid sodium (600 mg/l) and 88% (v/v) 100-mM phosphate buffer adjusted to pH 5.68. The pump flow rate was 0.23 ml/min. Chromatograms were recorded and analyzed by a laboratory computer connected with an A–D converter (Power Chrom EPC-500, Eicom). NE concentrations were determined by measuring the peak areas. The absolute detection limit of NE was 0.1 pg per injection (signal-to-noise ratio = 3).

Dialysate myoglobin concentrations were measured by the Cardiac Reader system (Roche Diagnostics). Single-use immunochemical test strips were used in the Cardiac Reader system. When a sample was added to the test well, the sample migrated along the strip due to capillary action, and myoglobin combined with two specific monoclonal antibodies. The resulting sandwich complex was immobilized by streptavidin in a stripe along the read window, producing a reddish line with an intensity related to myoglobin concentration. The CCD (Charge Coupled Device) camera quantified the intensity of the signal line and control line on the immunochemical test strips via reflectance measurements. The reflectance measurements were then converted into myoglobin concentration using electronically stored lot-specific calibration curves. The measuring range was between 30 and 700 ng/ml (Ambrose et al. 2002). When dialysate myoglobin concentrations were expected to be higher than 700 ng/ml, dialysate samples were diluted 10 or 100 times with saline.

Experimental protocols

Time courses of dialysate NE and myoglobin concentrations during acute myocardial ischemia/reperfusion (n = 6, vehicle group)

We examined the time courses of dialysate NE and myoglobin concentrations during 30 min of ischemia followed by 30 min of reperfusion. After 15-min baseline sampling, the main branch of the LCX was occluded for 30 min and then was released. Four consecutive 15-min

dialysate samples were collected during coronary occlusion (30 min) and reperfusion (30 min).

Influence of cariporide on time courses of dialysate NE and myoglobin concentrations during acute myocardial ischemia/reperfusion (n = 6, cariporide-treated group)

We examined the effects of cariporide on NE and myoglobin releases during ischemia/reperfusion. Ten-mg powder of cariporide (Santa Cruz Biotechnology, Inc., CA, USA) was dissolved in 10-ml saline. After 15-min baseline sampling, cariporide of 0.3 mg/kg, which reportedly caused a sufficient reduction in infarct mass (Linz et al., 1998), was injected intravenously before coronary occlusion. The LCX occlusion and reperfusion were performed as described in the vehicle group, and four consecutive dialysate samples were collected.

Statistical methods

All data are presented as mean ± standard error. For each protocol, heart rate and mean arterial pressure were compared by one-way repeated measures analysis of variance followed by a Dunnett's test versus baseline. After logarithmic transformation, dialysate NE and myoglobin concentrations were compared by one-way repeated measures analysis of variance followed by a Dunnett's test versus baseline. The differences between two groups were compared by unpaired *t*-test. Statistical significance was defined as $P < 0.05$.

Results

Time courses of heart rate and mean arterial pressure

The time courses of heart rate and mean arterial pressure during myocardial ischemia/reperfusion are shown in Table 1. In the vehicle group, coronary occlusion did not affect heart rate or mean arterial pressure. After reperfusion, heart rate decreased significantly but slightly to 266 ± 6 bpm at 7.5 min (compared with baseline: 277 ± 5 bpm; $P < 0.05$) and 265 ± 4 bpm at 22.5 min of reperfusion ($P < 0.05$ vs. baseline). In the cariporide-treated group, heart rate and mean arterial pressure did not change throughout ischemia and reperfusion.

There were no significant differences between the vehicle and cariporide-treated groups in heart rate and mean arterial pressure throughout the experiment.

Time course of dialysate NE concentration

Time course of dialysate NE concentration is shown in Fig. 1. In some baseline samples, dialysate NE concentrations were below the detection limit (0.1 pg/30-μl injection). For statistical analysis, baseline values were represented by the detection limit of 3.7 pg/ml.

In the vehicle group, dialysate NE concentration increased to 7251 ± 1891 pg/ml at 0–15 min of ischemia ($P < 0.01$ vs. baseline), reaching a peak of 56,586 ± 10,972 pg/ml at 15–30 min of ischemia ($P < 0.01$ vs. baseline). After reperfusion, dialysate NE concentration decreased to 16,837 ± 3906 pg/ml at 0–15 min ($P < 0.01$ vs. baseline), and further to 675 ± 243 pg/ml at 15–30 min of reperfusion ($P < 0.01$ vs. baseline).

In the cariporide-treated group, dialysate NE concentration increased significantly to 1174 ± 273 pg/ml at 0–15 min of ischemia ($P < 0.01$ vs. baseline), reaching a peak of 29,278 ± 4138 pg/ml at 15–30 of ischemia ($P < 0.01$ vs. baseline). After reperfusion, dialysate NE concentration decreased to 11,913 ± 3145 pg/ml at 0–15 min ($P < 0.01$ vs. baseline), and further to 414 ± 133 pg/ml at 15–30 min of reperfusion ($P < 0.01$ vs. baseline).

Dialysate NE concentrations in the cariporide-treated group were significantly lower than those in the vehicle group during ischemia ($P < 0.01$ at 0–15 min and $P < 0.05$ at 15–30 min). However, there were no significant differences in dialysate NE concentration between two groups during reperfusion.

Table 1
Heart rate and mean arterial pressure during acute myocardial ischemia/reperfusion.

	Baseline	Ischemia 7.5 min	Ischemia 22.5 min	Reperfusion 7.5 min	Reperfusion 22.5 min
Vehicle (n = 6)					
Heart rate (bpm)	277 ± 5	269 ± 6	267 ± 4	266 ± 6*	265 ± 4*
Mean arterial pressure (mm Hg)	84 ± 4	80 ± 5	82 ± 5	82 ± 6	82 ± 6
Cariporide (n = 6)					
Heart rate (bpm)	274 ± 4	278 ± 6	276 ± 5	271 ± 6	269 ± 3
Mean arterial pressure (mm Hg)	80 ± 2	85 ± 3	85 ± 3	78 ± 2	75 ± 1

Data are expressed as mean ± standard error. *P < 0.05 by ANOVA followed by Dunnett's test versus baseline.

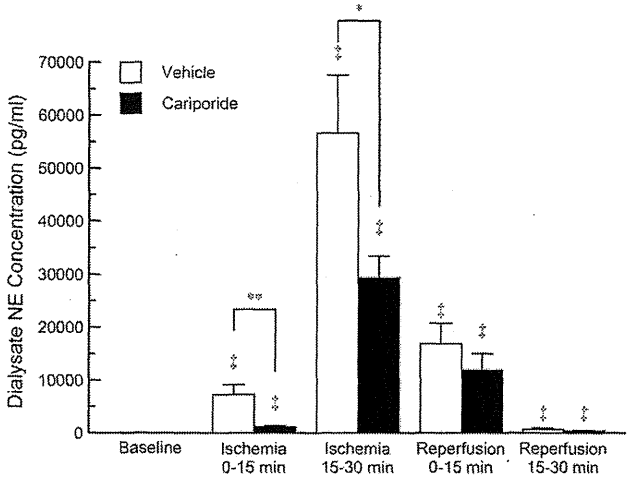

Fig. 1. Time courses of dialysate norepinephrine (NE) concentration during 30 min of ischemia followed by 30 min of reperfusion. Each dialysate sample was collected over a period of 15 min. Data are expressed as mean ± standard error. ‡P < 0.01, by ANOVA followed by Dunnett's test versus baseline; *P < 0.05 and **P < 0.01, by unpaired *t*-test.

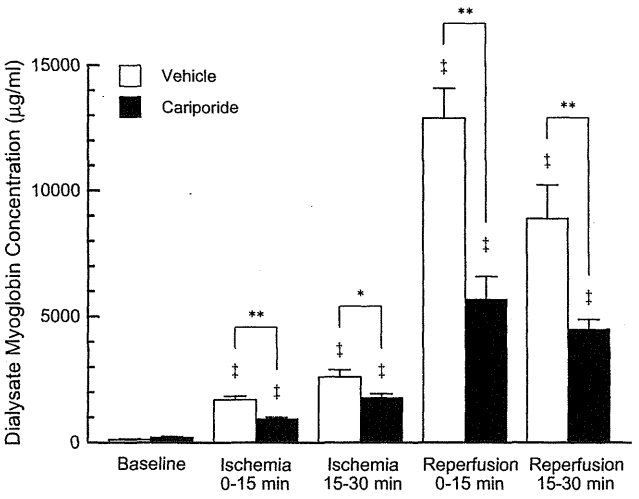

Fig. 2. Time courses of dialysate myoglobin concentration during 30 min of ischemia followed by 30 min of reperfusion. Each dialysate sample was collected over a period of 15 min. Data are expressed as mean ± standard error. ‡P < 0.01, ANOVA followed by Dunnett's test versus baseline; *P < 0.05 and **P < 0.01, by unpaired t test.

Time course of dialysate myoglobin concentration

Time course of dialysate myoglobin concentration is shown in Fig. 2. In the vehicle group, dialysate myoglobin concentration increased significantly from 128 ± 25 ng/ml at baseline to 1717 ± 137 ng/ml at 0–15 min of ischemia ($P < 0.01$ vs. baseline), and further to 2630 ± 262 ng/ml at 15–30 min of ischemia ($P < 0.01$ vs. baseline). After reperfusion, dialysate myoglobin concentration reached a peak of 12,887 ± 1186 ng/ml at 0–15 min ($P < 0.01$ vs. baseline), followed by a gradual decline (8903 ± 1317 ng/ml at 15–30 of after reperfusion, $P < 0.01$ vs. baseline).

In the cariporide-treated group, dialysate myoglobin concentration increased significantly from 218 ± 38 ng/ml at baseline to 943 ± 80 ng/ml at 0–15 min of ischemia ($P < 0.01$ vs. baseline), and further to 1798 ± 169 ng/ml at 15–30 min of ischemia ($P < 0.01$ vs. baseline). After reperfusion, dialysate myoglobin concentration reached a peak of 5690 ± 924 ng/ml at 0–15 min ($P < 0.01$ vs. baseline), followed by a gradual decline (4500 ± 395 ng/ml at 15–30 min of reperfusion, $P < 0.01$ vs. baseline).

Dialysate myoglobin concentrations in the cariporide-treated group were significantly lower than those in the vehicle group throughout ischemia/reperfusion ($P < 0.01$ at 0–15 min of ischemia, $P < 0.05$ at 15–30 min of ischemia, $P < 0.01$ at 0–15 min of reperfusion and $P < 0.01$ at 15–30 min of reperfusion).

Discussion

The present study demonstrated that intravenous injection of cariporide before coronary occlusion significantly reduced interstitial myoglobin levels during ischemia/reperfusion, and suppressed NE release from sympathetic nerve endings during ischemia but not during reperfusion.

NHE-1 inhibition and NE release

During acute myocardial ischemia, excessive NE release from sympathetic nerve endings and reduced NE reuptake into nerve endings may cause functional damages such as life-threatening arrhythmia. There are two major processes of NE release from sympathetic nerve endings. Under physiological conditions, NE is mainly released via Ca^{2+}-dependent exocytosis. In myocardial ischemia, however, the predominant process of NE release is Ca^{2+}-independent nonexocytosis via NET (Kurz et al., 1995). Physiologically, NET relocates NE within the synaptic cleft into the axoplasm, where NE is taken up into storage vesicles or degraded by monoamine oxidase. The NE vesicular storage depends on the pH gradient across the vesicular membrane maintained by an ATP-dependent H^+ pump. Increase in H^+ due to lowered pH as well as ATP depletion during ischemia leads to an increase in free axoplasmic NE (Leineweber et al., 2007), and activates the influx of Na^+ via NHE-1. Since the direction of NET-mediated transport depends on the Na^+ gradient across the membrane of sympathetic nerve terminals (Schömig et al., 1991), a rise in axoplasmic Na^+ concentration during ischemia diminishes the inward transport and favors the outward transport of NE, causing excessive Ca^{2+}-independent nonexocytotic NE release (Leineweber et al., 2007). Thus, by inhibiting NHE-1, cariporide may reduce the influx of Na^+ and suppress nonexocytotic NE release during ischemia. The present study proved that cariporide significantly reduces interstitial NE levels during ischemia. Therefore, cariporide may suppress functional damage caused by excessive NE release during ischemia.

This study also provided important evidence that cariporide does not reduce NE release during reperfusion. Thus, the effects of cariporide against excessive NE release may be limited to the ischemic period but not during reperfusion. This may be a reason why several clinical trials failed to prove the cardioprotective effects of NHE-1 inhibitors administered shortly before reperfusion. In the ESCAMI (Evaluation of the Safety and Cardioprotective Effects of Eniporide in Acute Myocardial Infarction) trial, administration of eniporide before reperfusion in patients with acute myocardial infarction did not improve clinical outcomes (death, cardiogenic shock, heart failure, life-threatening arrhythmias) (Zeymer et al., 2001). A previous study demonstrated that myocardial interstitial NE level decreased while dihydroxyphenylglycol (a metabolite of NE) level increased rapidly after reperfusion (Akiyama and Yamazaki, 2001). Thus, metabolites of catecholamine may also be associated with functional damage during reperfusion. Further investigations are necessary to clarify the effects of NHE-1 inhibitors on functional damage during reperfusion.

NHE-1 inhibition and myoglobin release

During myocardial ischemia, anaerobic glycolysis and ATP degradation produce H^+ that activates the influx of Na^+ via NHE-1. However, Na^+ efflux is attenuated because the Na^+/K^+-ATPase is inhibited during ischemia. Therefore, the net result enhanced Na^+ influx and reduced Na^+ efflux. An accumulation of intracellular Na^+ induces cytoplasmic Ca^{2+} overload via reverse-mode Na^+/Ca^{2+} exchanger, resulting in structural damage during myocardial ischemia/reperfusion (Leineweber et al., 2007). Therefore, cariporide may reduce Na^+ influx and suppress Ca^{2+} overload, resulting in the reduction of structural damage indicated by myoglobin release. Furthermore, several possible mechanisms of cardioprotective effects of cariporide have already been suggested. Nuñez et al. (2011) reported that attenuation of calcium-induced permeability transition pore opening after protein kinase C (PKC)-mediated mitochondrial ATP-sensitive potassium channel activation was a crucial step for the cardioprotective effects of cariporide. On the other hand, Ajiro et al. (2011) reported that platelet-activating factor (PAF) stimulated cardiac NHE-1 via the PAF receptor and signal relay required participation of the mitogen-activated protein kinase cascade. They also reported that PKC might not be involved in the stimulation of NHE-1 because PKC inhibitors did not significantly reduce the responses to PAF. Further investigations are clearly needed to identify the mechanisms.

Létienne et al. (2006) reported that cariporide significantly reduced plasma myoglobin level that strongly correlated with myocardial necrosis. However, we have previously demonstrated that plasma myoglobin level responds less sensitively than myocardial interstitial myoglobin level monitored by cardiac microdialysis (Kitagawa et al., 2005). Although a significant change in plasma myoglobin level occurs at 45–60 min after coronary occlusion in a rabbit ischemia model (Kitagawa et al., 2005), the myocardial microdialysis technique can detect a significant change in interstitial myoglobin level within 15 min after occlusion. The present study demonstrated that cariporide reduced interstitial myoglobin level from the early phase (0–15 min) of myocardial ischemia and this effect was sustained even after reperfusion was started. Several experimental studies have reported that preconditioning with cariporide salvages myocytes and reduces the release of cardiac-specific enzymes (Cun et al., 2007; Haist et al., 2003). Furthermore, the GUARDIAN (Guard During Ischemia Against Necrosis) trial revealed a significant correlation between elevated creatine kinase myocardial band (CK-MB) during the initial 48 h after coronary artery bypass grafting (CABG) and significantly increased six-month mortality (Gavard et al., 2003). A subgroup analysis of the GUARDIAN data revealed that a 120-mg dose of cariporide significantly reduced the combined incidence of death and myocardial infarction in patients undergoing high-risk CABG surgery, and that this benefit was sustained for 6 months (Boyce et al., 2003). Therefore, a reduction in the release of cardiac enzymes after reperfusion may have a close relation to the improvement of surgical outcomes. In the present study, cariporide also suppressed peak interstitial myoglobin level after reperfusion. Thus, cariporide administration before ischemia may be an effective cardioprotective strategy against structural damage during ischemia/reperfusion.

On the other hand, several studies have demonstrated that treatment with cariporide shortly before reperfusion does not

reduce infarct size (Miura et al., 1997; Reffelmann and Kloner, 2003). Klein et al. (2000) reported that the reduction of infarct size was detectable only when cariporide was infused during the first 30 min after ischemia. In their study, cariporide infused after 45 min of ischemia until 10 min of reperfusion failed to reduce infarct size. In the ESCAMI trial, pretreatment with eniporide in patients undergoing reperfusion therapy for acute ST-elevation myocardial infarction did not reduce infarct size assessed by cardiac enzyme release (Zeymer et al., 2001). The present study revealed that pretreated cariporide significantly reduced interstitial myoglobin level from the very early phase after myocardial ischemia. This fact may be a reason why cariporide should be administered before ischemia to exert its cardioprotective effects. Thus, the reduction of interstitial myoglobin level during reperfusion observed in the present study may reflect amelioration of structural damage caused by ischemia and not necessarily the damage induced by reperfusion. Nevertheless, cariporide has a certain cardioprotective effect against structural damage during ischemia and reperfusion.

Methodological considerations

The responses of heart rate and arterial pressure to myocardial ischemia/reperfusion were small in the present study. Because Kashihara et al. (2004) reported that Bezold–Jarisch (B–J) reflex induced by phenylbiguanide blunted arterial baroreflex via the shift of the neural arc toward lower sympathetic nerve activity, small responses in heart rate and arterial pressure might be due to weak B–J reflex during acute myocardial ischemia in rabbits.

Conclusions

Intravenous cariporide significantly reduced myocardial interstitial myoglobin level during ischemia/reperfusion and decreased NE release during ischemia. When administered before ischemia, treatment with cariporide may be an effective cardioprotective strategy against structural damage during ischemia/reperfusion and excessive NE release during ischemia.

Conflict of interest statement

The authors declare that there are no conflicts of interest.

Acknowledgment

This study was supported by a Medical Research Promotion Grant from the Takeda Science Foundation, Japan.

References

Ajiro Y, Saegusa N, Giles WR, Stafforini DM, Spitzer KW. Platelet-activating factor stimulates sodium–hydrogen exchange in ventricular myocytes. Am J Physiol Heart Circ Physiol 2011;301:H2395–401.
Akiyama T, Yamazaki T. Myocardial interstitial norepinephrine and dihydroxyphenylglycol levels during ischemia and reperfusion. Cardiovasc Res 2001;49:78–85.
Akiyama T, Yamazaki T, Ninomiya I. In vivo monitoring of myocardial interstitial norepinephrine by dialysis technique. Am J Physiol 1991;261:H1643–7.
Ambrose TM, Knight D, Neher J. The Cardiac Reader: A Platform for Quantitative Point-of-Care Cardiac Marker Determinations From Roche Diagnostics. Point of Care. 2002;1:50–3.
Avkiran M. Rational basis for use of sodium–hydrogen exchange inhibitors in myocardial ischemia. Am J Cardiol 1999;83:10G–7G.
Avkiran M. Basic biology and pharmacology of the cardiac sarcolemmal sodium/hydrogen exchanger. J Card Surg 2003;18(Suppl. 1):3–12.
Boyce SW, Bartels C, Bolli R, Chaitman B, Chen JC, Chi E, et al. Impact of sodium–hydrogen exchange inhibition by cariporide on death or myocardial infarction in high-risk CABG surgery patients: results of the CABG surgery cohort of the GUARDIAN study. J Thorac Cardiovasc Surg 2003;126:420–7.
Cun L, Ronghua Z, Bin L, Jin L, Shuyi L. Preconditioning with Na^+/H^+ exchange inhibitor HOE642 reduces calcium overload and exhibits marked protection on immature rabbit hearts. ASAIO J 2007;53:762–5.
Fliegel L. The Na^+/H^+ exchanger isoform 1. Int J Biochem Cell Biol 2005;37:33–7.
Gavard JA, Chaitman BR, Sakai S, Stocke K, Danchin N, Erhardt L, et al. Prognostic significance of elevated creatine kinase MB after coronary bypass surgery and after an acute coronary syndrome: results from the GUARDIAN trial. J Thorac Cardiovasc Surg 2003;126:807–13.
Haist JV, Hirst CN, Karmazyn M. Effective protection by NHE-1 inhibition in ischemic and reperfused heart under preconditioning blockade. Am J Physiol Heart Circ Physiol 2003;284:H798–803.
Kashihara K, Kawada T, Li M, Sugimachi M, Sunagawa K. Bezold–Jarisch reflex blunts arterial baroreflex via the shift of neural arc toward lower sympathetic nerve activity. Jpn J Physiol 2004;54:395–404.
Kitagawa H, Yamazaki T, Akiyama T, Sugimachi M, Sunagawa K, Mori H. Microdialysis separately monitors myocardial interstitial myoglobin during ischemia and reperfusion. Am J Physiol Heart Circ Physiol 2005;289:H924–30.
Klein HH, Pich S, Bohle RM, Lindert-Heimberg S, Nebendahl K. Na^+/H^+ exchange inhibitor cariporide attenuates cell injury predominantly during ischemia and not at onset of reperfusion in porcine hearts with low residual blood flow. Circulation 2000;102:1977–82.
Kristo G, Yoshimura Y, Ferraris SP, Jahania SA, Mentzer Jr RM, Lasley RD. The preischemic combination of the sodium–hydrogen exchanger inhibitor cariporide and the adenosine agonist AMP579 acts additively to reduce porcine myocardial infarct size. J Am Coll Surg 2004;199:586–94.
Kurz T, Richardt G, Hagl S, Seyfarth M, Schömig A. Two different mechanisms of noradrenaline release during normoxia and simulated ischemia in human cardiac tissue. J Mol Cell Cardiol 1995;27:1161–72.
Leineweber K, Heusch G, Schulz R. Regulation and role of the presynaptic and myocardial Na^+/H^+ exchanger NHE1: effects on the sympathetic nervous system in heart failure. Cardiovasc Drug Rev 2007;25:123–31.
Létienne R, Bel L, Bessac AM, Denais D, Degryse AD, John GW, et al. Cardioprotection of cariporide evaluated by plasma myoglobin and troponin I in myocardial infarction in pigs. Fundam Clin Pharmacol 2006;20:105–13.
Linz W, Albus U, Crause P, Jung W, Weichert A, Schölkens BA, et al. Dose-dependent reduction of myocardial infarct mass in rabbits by the NHE-1 inhibitor cariporide (HOE642). Clin Exp Hypertens 1998;20:733–49.
Miura T, Ogawa T, Suzuki K, Goto M, Shimamoto K. Infarct size limitation by a new $Na(+)$-H^+ exchange inhibitor, HOE642: difference from preconditioning in the role of protein kinase C. J Am Coll Cardiol 1997;29:693–701.
Nuñez IP, Fantinelli J, Arbeláez LF, Mosca SM. Mitochondrial KATP channels participate in the limitation of infarct size by cariporide. Naunyn Schmiedebergs Arch Pharmacol 2011;383:563–71.
Reffelmann T, Kloner RA. Is microvascular protection by cariporide and ischemic preconditioning causally linked to myocardial salvage? Am J Physiol Heart Circ Physiol 2003;284:H1134–41.
Schömig A, Haass M, Richardt G. Catecholamine release and arrhythmias in acute myocardial ischaemia. Eur Heart J 1991;12(Suppl. F):38–47.
Zeymer U, Suryapranata H, Monassier JP, Opolski G, Davies J, Rasmanis G, et al. The Na^+/H^+ exchange inhibitor eniporide as an adjunct to early reperfusion therapy for acute myocardial infarction. Results of the evaluation of the safety and cardioprotective effects of eniporide in acute myocardial infarction (ESCAMI) trial. J Am Coll Cardiol 2001;38:1644–50.

Autonomic Neuroscience: Basic and Clinical 187 (2015) 84–87

Contents lists available at ScienceDirect

Autonomic Neuroscience: Basic and Clinical

journal homepage: www.elsevier.com/locate/autneu

Short communication

Guanfacine enhances cardiac acetylcholine release with little effect on norepinephrine release in anesthetized rabbits

Shuji Shimizu [a,*], Toru Kawada [a], Tsuyoshi Akiyama [b], Michael James Turner [a], Toshiaki Shishido [c], Atsunori Kamiya [a], Mikiyasu Shirai [b], Masaru Sugimachi [a]

[a] Department of Cardiovascular Dynamics, National Cerebral and Cardiovascular Center, Osaka 565-8565, Japan
[b] Department of Cardiac Physiology, National Cerebral and Cardiovascular Center, Osaka 565-8565, Japan
[c] Department of Research Promotion and Management, National Cerebral and Cardiovascular Center, Osaka 565-8565, Japan

ARTICLE INFO

Article history:
Received 10 September 2014
Received in revised form 12 November 2014
Accepted 25 November 2014

Keywords:
Guanfacine
α_2-Adrenergic agonist
Acetylcholine
Norepinephrine
Microdialysis

ABSTRACT

An α_{2A}-adrenergic agonist guanfacine improves autonomic imbalance in attention-deficit hyperactivity disorder, suggesting that it may be useful to correct autonomic imbalance in chronic heart failure (CHF) patients. To investigate the effects of guanfacine on cardiac autonomic nerve activities, a microdialysis technique was applied to anesthetized rabbit heart. Acetylcholine (ACh) and norepinephrine (NE) concentrations in atrial dialysates were measured as indices of cardiac autonomic nerve activities. Guanfacine at a dose of 100 μg/kg significantly decreased heart rate and increased dialysate ACh concentration without decreasing sympathetic NE release. Guanfacine may be useful for vagal activation therapy in CHF patients.

1. Introduction

Autonomic imbalance with activation of sympathetic nerve system and suppression of vagal nerve system causes progression of heart failure. Vagal activation has recently become a therapeutic option to correct autonomic imbalance in patients with chronic heart failure (CHF) (De Ferrari and Schwartz, 2011). Currently a clinical trial of electrical vagal nerve stimulation (VNS) for CHF is on-going (Hauptman et al., 2012). We have already demonstrated that an α_2-adrenergic agonist, medetomidine, activates cardiac vagal nerve (Shimizu et al., 2012), suggesting that a class of α_2-adrenergic agonists may correct the autonomic imbalance in CHF patients. However, medetomidine also has a sedative anesthetic effect. This may prevent widespread clinical use of medetomidine or dexmedetomidine in CHF treatment. Furthermore, severe hypotension during medetomidine treatment may also limit its clinical use.

Guanfacine, a selective α_{2A}-adrenergic agonist, has recently been approved for the treatment of attention-deficit hyperactivity disorder (ADHD) (Biederman et al., 2008). A systematic review suggests that children with unmedicated ADHD experience lower levels of cardiac vagal control than healthy controls, and guanfacine partly corrects this autonomic imbalance in ADHD patients (Rash and Aguirre-Camacho, 2012). Furthermore, Yamazaki et al. (2005) have reported that guanfacine improves sympathovagal imbalance related to rapid-eye-movement (REM)/non-REM ultradian sleep rhythm in CHF patients. Thus, guanfacine may be a potential pharmacological agent for vagal activation therapy in CHF patients. To clarify the effects of guanfacine on cardiac autonomic nerve activities, we applied a microdialysis technique to rabbit heart.

2. Materials and methods

2.1. Surgical preparation

Animal care was provided in accordance with the *Guiding Principles for the Care and Use of Animals in the Field of Physiological Sciences* published by the Physiological Society of Japan. All protocols were approved by the Animal Subject Committee of the National Cerebral and Cardiovascular Center. Seven Japanese white rabbits weighing 2.4 to 2.8 kg were used in this study. Anesthesia was initiated by an intravenous injection of pentobarbital sodium (50 mg/kg) via the marginal ear vein, and then maintained at an appropriate level by continuous intravenous infusion of α-chloralose and urethane (16 $mg \cdot kg^{-1} \cdot h^{-1}$ and 100 $mg \cdot kg^{-1} \cdot h^{-1}$, respectively). Adequate anesthesia level was confirmed by loss of the ear pinch response. The animals were ventilated mechanically with a mixture of room air and oxygen (respiratory rate, 30 cycles/min; volume, 15 ml/kg). A fluid-filled catheter was inserted

* Corresponding author at: Department of Cardiovascular Dynamics, National Cerebral and Cardiovascular Center, 5-7-1 Fujishiro-dai, Suita, Osaka 565-8565, Japan. Tel.: +81 6 6833 5012; fax: +81 6 6835 5403.
E-mail address: shujismz@ri.ncvc.go.jp (S. Shimizu).

http://dx.doi.org/10.1016/j.autneu.2014.11.010
1566-0702/

into the femoral artery to monitor systemic arterial pressure. Esophageal temperature was maintained between 38 and 39 °C using a heating pad.

With the animal in supine position, a right lateral thoracotomy was performed and the right 3rd to 5th ribs were partially resected to expose the heart. After pericardium incision, a dialysis probe was implanted as described in *Dialysis Technique* below. Three stainless steel electrodes were attached around the thoracotomy incision for monitoring body surface electrocardiogram (ECG). The ECG was connected to a cardiotachometer and heart rate was recorded.

At the end of the experiment, the animal was euthanized by injecting an overdose of pentobarbital sodium. In the postmortem examination, the inside of the resected atrial wall was observed macroscopically to confirm that the dialysis membrane was implanted totally within the atrial myocardium.

2.2. Dialysis technique

The materials and properties of the dialysis probe have been described previously (Shimizu et al., 2009, 2010). A dialysis fiber of semipermeable membrane (length 4 mm, PAN-1200; Asahi Chemical, Tokyo, Japan) was attached at both ends to polyethylene tubes (length 25 cm). The dialysis probe was implanted into the right atrial myocardium near the sinoatrial node, and was perfused with Ringer's solution containing a cholinesterase inhibitor, eserine (100 μM), at a speed of 2 μl/min using a microinjection pump (CMA/102, Carnegie Medicin, Sweden). Experimental protocol was started 2 h after implantation. Eight microliters of phosphate buffer (pH 3.5) was added to each sample tube before dialysate sampling, and each dialysate sampling period was set at 20 min (1 sample volume = 40 μl). Dialysate acetylcholine (ACh) and norepinephrine (NE) concentrations were analyzed separately by high performance liquid chromatography (Akiyama et al., 1991, 1994).

2.3. Experimental protocols

We investigated the effects of intravenous guanfacine on vagal ACh and sympathetic NE releases into the myocardium. Baseline dialysate samples were collected over 20 min before the injection of guanfacine. A low dose (10 μg/kg) of guanfacine (Sigma-Aldrich Co. LLC., St. Louis, MO, USA) was injected intravenously via the femoral vein. After approximately 20-min hemodynamic stabilization, dialysate was sampled for 20 min (40 μl). Thereafter, a high dose (100 μg/kg) of guanfacine was injected intravenously and another 20-min dialysate sample was collected after 20-min hemodynamic stabilization. Finally, bilateral cervical vagotomy was performed and a 20-min dialysate sample was collected 5 min after vagotomy taking into account the dead space between the dialysate membrane and the sample tube.

2.4. Statistical analysis

All data are presented as mean ± standard error. Heart rate and mean arterial pressure were compared by one-way repeated measures analysis of variance (ANOVA) followed by a Dunnett's test against baseline. After logarithmic transformation, dialysate ACh and NE concentrations were also compared by one-way repeated measures ANOVA followed by a Dunnett's test against baseline. Differences were considered significant at $P < 0.05$.

3. Results

Intravenous guanfacine at a dose of 10 μg/kg did not affect heart rate (264 ± 8 bpm at baseline to 243 ± 7 bpm, not significant) and mean arterial pressure (88 ± 2 mm Hg at baseline to 77 ± 2 mm Hg, not significant) (Fig. 1A and B). Dialysate ACh and NE concentrations at baseline were 6.7 ± 1.2 nM and 193 ± 22 pM, respectively (Fig. 2A and B). Intravenous injection of 10 μg/kg of guanfacine did not affect dialysate ACh and NE concentrations (7.3 ± 1.2 nM and 156 ± 23 pM, respectively).

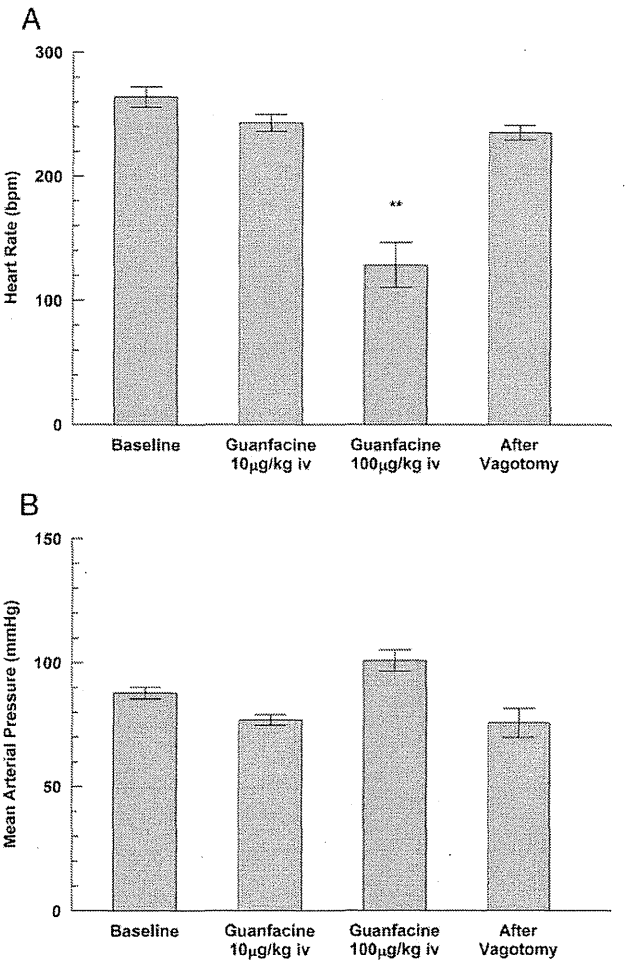

Fig. 1. Heart rate (A) and mean arterial pressure (B) at baseline, after intravenous injection (iv.) of guanfacine, and after bilateral cervical vagaotomy. **, $P < 0.01$ by Dunnett's test against baseline.

Intravenous guanfacine at a dose of 100 μg/kg significantly decreased heart rate to 128 ± 18 bpm ($P < 0.01$ vs. baseline), but had no effect on mean arterial pressure (101 ± 4 mm Hg, not significant vs. baseline) (Fig. 1B). Intravenous injection of 100 μg/kg of guanfacine significantly increased dialysate ACh concentration to 41.7 ± 8.4 nM ($P < 0.01$ vs. baseline) (Fig. 2A), whereas this dose of guanfacine did not affect dialysate NE concentration (172 ± 36 pM, not significant vs. baseline) (Fig. 2B). Heart rate and dialysate ACh concentration recovered to the baseline levels immediately after vagotomy (235 ± 6 bpm and 7.8 ± 1.2 nM, respectively).

4. Discussion

Guanfacine, a selective α_{2A}-adrenergic agonist, was previously used as a centrally acting antihypertensive drug because study indicated that guanfacine acted on the central nervous system and suppressed sympathetic nerve activity (Scholtysik, 1986). Although α_{2A}-adrenergic receptor subtype plays a principal role in central hypotensive effects of α_2-adrenergic agonists (MacMillan et al, 1996), the sympatholytic effect of guanfacine seems to be weaker than those of other α_2-adrenergic agonists. Our previous study demonstrated that 10 and 100 μg/kg of medetomidine, another α_2-adrenergic agonist, significantly decreased sympathetic NE release to the heart (Shimizu et al., 2012).

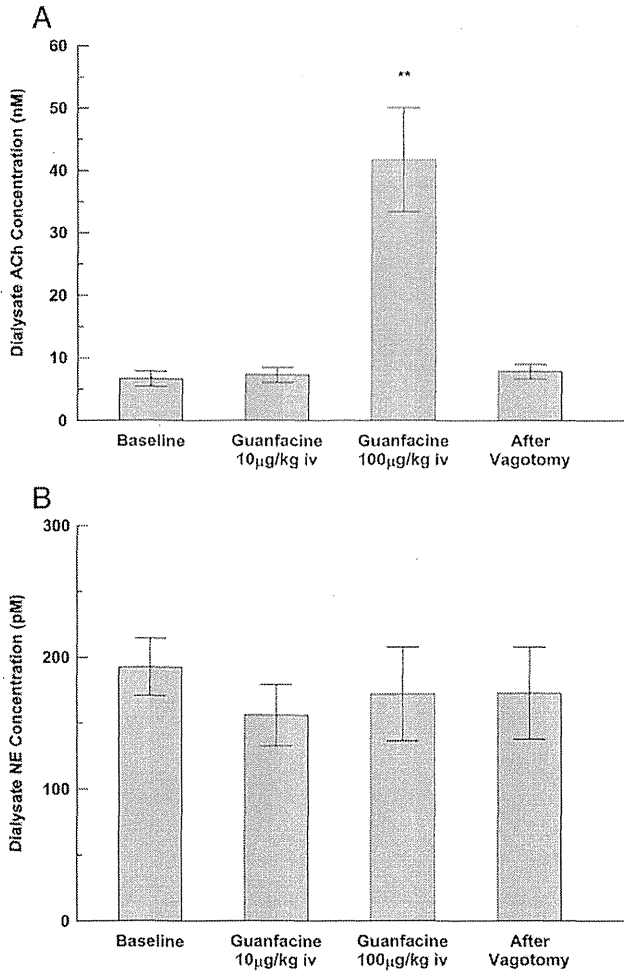

Fig. 2. Dialysate acetylcholine (ACh, A) and norepinephrine (NE, B) concentrations at baseline, after intravenous injection (iv.) of guanfacine and after bilateral cervical vagotomy. **, $P < 0.01$ by Dunnett's test against baseline.

In the present study, 10 μg/kg of guanfacine tended to decrease sympathetic NE release ($P = 0.08$), but this decrease did not reach a statistical significance. One-hundred microgram per kilogram of guanfacine did not affect sympathetic NE release. This little effect on sympathetic NE release may be due to the structure of guanfacine. Other α_2-adrenergic agonists such as medetomidine, dexmedetomidine and clonidine have an imidazole structure, and act on imidazoline receptors as well as α_2-adrenergic receptors. Recent study suggests that an imidazoline receptor agonist, moxonidine, centrally suppresses sympathetic nerve activity (Peng et al., 2009). Thus, the action of other α_2-adrenergic agonists on imidazoline receptors may contribute to the strong sympatholytic effect exhibited by these agents. On the other hand, guanfacine has no imidazole structure. Thus, the effect of guanfacine on sympathetic nerve activity may be totally dependent on its action on α_2-adrenergic receptor, which would account for the relatively weak effect. Although further investigations are necessary to explain the relatively weak effect on sympathetic nerve activity, this mechanism may be a reason why guanfacine is regarded as a second-line drug for hypertension, compared to other drugs such as calcium antagonists and angiotensin II receptor blockers (Sorkin and Heel, 1986).

The effect of guanfacine on vagal nerve activity has remained unclear. However, several studies suggest that α_2-adrenergic agonists may activate cardiac vagal nerve. Philbin et al. (2010) showed that clonidine significantly inhibited GABAergic neurotransmission to cardiac vagal neurons in the nucleus ambiguus. Inhibition of GABAergic neurotransmission may increase vagal activity to the heart. Kamibayashi et al. (1995) reported that the antidysrhythmic effect of dexmedetomidine was abolished in both vagotomized and atropine-treated dogs. Yamazaki et al. (2005) reported that guanfacine increased the power of high frequency component of heat rate variability during sleep. However, these findings are no more than indirect evidence that α_2-adrenergic agonists may activate cardiac vagal nerve. No direct evidence was available to confirm whether α_2-adrenergic agonists are able to activate cardiac vagal nerve, because it was difficult to selectively monitor cardiac vagal nerve activity in the past. Using a cardiac microdialysis technique, we have already reported that medetomidine, an α_2-adrenergic agonist, enhances vagal ACh release to the heart (Shimizu et al., 2012). Thus, the cardiac microdialysis technique may be the only method that allows selective monitoring of cardiac vagal nerve activity, apart from a single cardiac vagal fiber recording method reported previously (Cerati and Schwartz, 1991). In the present study using this technique, we demonstrated that 100 μg/kg of guanfacine increased vagal ACh release to the heart and this increase was abolished by bilateral cervical vagotomy. This result is direct evidence that guanfacine can activate cardiac vagal nerve. Since α_2-adrenergic receptors are known to be distributed in the nucleus tractus solitaries and nucleus ambiguus (Philbin et al., 2010; Robertson and Leslie, 1985), guanfacine may act on these nuclei to increase vagal ACh release to the heart.

The present study suggests that guanfacine has several advantages in various clinical settings, compared to other α_2-adrenergic agonists such as medetomidine. First, guanfacine causes less sedation than other α_2-adrenergic agonists (Scholtysik, 1986). Second, although guanfacine has been reported to cause hypotension, the changes in blood pressure are small to moderate and not clinically significant (Biederman et al., 2008). The dose of guanfacine (100 μg/kg) used in the present study is almost equivalent to the daily dose (80 to 120 μg/kg/day) for the treatment of ADHD in the clinical setting. However, this high dose of guanfacine did not cause severe hypotension. Thus, guanfacine may be a more favorable agent for vagal activation therapy in CHF patients compared to other α_2-adrenergic agonists.

This study has several methodological considerations. First, this experiment was performed under α-chloralose and urethane anesthesia. Because chloralose–urethane anesthesia reduced cardiac vagal efferent activity (Korner et al., 1968), vagotonic effect of guanfacine might have been more easily demonstrated compared with conscious conditions. On the other hand, we have already reported that an α_2-adrenergic agonist, medetomidine, enhances vagal ACh release through the modulation of baroreflex (Shimizu et al., 2012). Therefore, we think that vagal activation of guanfacine may be a direct action to the central nervous system. However, further investigations are necessary to clarify the mechanism of guanfacine-induced vagal activation. Second, the dose-dependent response of guanfacine was not examined in random order because plasma half-life of guanfacine was reported to be over 2 h (Barber and Reid, 1982). Therefore, 10 μg/kg of guanfacine might have partly affected the results of 100 μg/kg of guanfacine.

In conclusion, intravenous guanfacine at a dose of 100 μg/kg significantly enhanced vagal ACh release to the heart with no significant effect on sympathetic NE release. This vagotonic effect of guanfacine may be beneficial for vagal activation therapy in CHF patients.

Acknowledgments

This study was supported by the Grant-in-Aid for Scientific Research (23390415, 23592319) promoted by the Ministry of Education, Culture, Sports, Science, and Technology of Japan, and by the Medical Research Promotion Grant from the Takeda Science Foundation, Japan.

References

Akiyama, T., Yamazaki, T., Ninomiya, I., 1991. In vivo monitoring of myocardial interstitial norepinephrine by dialysis technique. Am. J. Physiol. 261, H1643–H1647.
Akiyama, T., Yamazaki, T., Ninomiya, I., 1994. In vivo detection of endogenous acetylcholine release in cat ventricles. Am. J. Physiol. 266, H854–H860.

Barber, N.D., Reid, J.L., 1982. Comparison of the actions of centrally and peripherally administered clonidine and guanfacine in the rabbit: investigation of the differences. Br. J. Pharmacol. 77, 641–647.
Biederman, J., Melmed, R.D., Patel, A., McBurnett, K., Konow, J., Lyne, A., Scherer, N., SPD503 Study Group, 2008. A randomized, double-blind, placebo-controlled study of guanfacine extended release in children and adolescents with attention-deficit/hyperactivity disorder. Pediatrics 121, e73–84.
Cerati, D., Schwartz, P.J., 1991. Single cardiac vagal fiber activity, acute myocardial ischemia, and risk for sudden death. Circ. Res. 69, 1389–1401.
De Ferrari, G.M., Schwartz, P.J., 2011. Vagus nerve stimulation: from pre-clinical to clinical application: challenges and future directions. Heart Fail. Rev. 16, 195–203.
Hauptman, P.J., Schwartz, P.J., Gold, M.R., Borggrefe, M., Van Veldhuisen, D.J., Starling, R.C., Mann, D.L., 2012. Rationale and study design of the increase of vagal tone in heart failure study: INOVATE-HF. Am. Heart J. 163 954-962.e1.
Kamibayashi, T., Hayashi, Y., Mammoto, T., Yamatodani, A., Sumikawa, K., Yoshiya, I., 1995. Role of the vagus nerve in the antidysrhythmic effect of dexmedetomidine on halothane/epinephrine dysrhythmias in dogs. Anesthesiology 83, 992–999.
Korner, P.I., Uther, J.B., White, S.W., 1968. Circulatory effects of chloralose–urethane and sodium pentobarbitone anaesthesis in the rabbit. J. Physiol. 199, 253–265.
MacMillan, L.B., Hein, L., Smith, M.S., Piascik, M.T., Limbird, L.E., 1996. Central hypotensive effects of the alpha2a-adrenergic receptor subtype. Science 273, 801–803.
Peng, J., Wang, Y.K., Wang, L.G., Yuan, W.J., Su, D.F., Ni, X., Deng, X.M., Wang, W.Z., 2009. Sympathoinhibitory mechanism of moxonidine: role of the inducible nitric oxide synthase in the rostral ventrolateral medulla. Cardiovasc. Res. 84, 283–291.
Philbin, K.E., Bateman, R.J., Mendelowitz, D., 2010. Clonidine, an alpha2-receptor agonist, diminishes GABAergic neurotransmission to cardiac vagal neurons in the nucleus ambiguus. Brain Res. 1347, 65–70.
Rash, J.A., Aguirre-Camacho, A., 2012. Attention-deficit hyperactivity disorder and cardiac vagal control: a systematic review. Atten. Deficit Hyperact. Disord. 4, 167–177.
Robertson, H.A., Leslie, R.A., 1985. Noradrenergic alpha 2 binding sites in vagal dorsal motor nucleus and nucleus tractus solitarius: autoradiographic localization. Can. J. Physiol. Pharmacol. 63, 1190–1194.
Scholtysik, G., 1986. Animal pharmacology of guanfacine. Am. J. Cardiol. 57, 13E–17E.
Shimizu, S., Akiyama, T., Kawada, T., Shishido, T., Yamazaki, T., Kamiya, A., Mizuno, M., Sano, S., Sugimachi, M., 2009. In vivo direct monitoring of vagal acetylcholine release to the sinoatrial node. Auton. Neurosci. 148, 44–49.
Shimizu, S., Akiyama, T., Kawada, T., Shishido, T., Mizuno, M., Kamiya, A., Yamazaki, T., Sano, S., Sugimachi, M., 2010. In vivo direct monitoring of interstitial norepinephrine levels at the sinoatrial node. Auton. Neurosci. 152, 115–118.
Shimizu, S., Akiyama, T., Kawada, T., Sata, Y., Mizuno, M., Kamiya, A., Shishido, T., Inagaki, M., Shirai, M., Sano, S., Sugimachi, M., 2012. Medetomidine, an α(2)-adrenergic agonist, activates cardiac vagal nerve through modulation of baroreflex control. Circ. J. 76, 152–159.
Sorkin, E.M., Heel, R.C., 1986. Guanfacine. A review of its pharmacodynamic and pharmacokinetic properties, and therapeutic efficacy in the treatment of hypertension. Drugs 31, 301–336.
Yamazaki, T., Asanoi, H., Ueno, H., Yamada, K., Takagawa, J., Kameyama, T., Hirai, T., Ishizaka, S., Nozawa, T., Inoue, H., 2005. Central sympathetic inhibition augments sleep-related ultradian rhythm of parasympathetic tone in patients with chronic heart failure. Circ. J. 69, 1052–1056.

Autonomic Neuroscience: Basic and Clinical 186 (2014) 62–68

Contents lists available at ScienceDirect

Autonomic Neuroscience: Basic and Clinical

journal homepage: www.elsevier.com/locate/autneu

Acute effects of arterial baroreflex on sympathetic nerve activity and plasma norepinephrine concentration

Toru Kawada [a,*], Tsuyoshi Akiyama [b], Shuji Shimizu [a], Yusuke Sata [a,c], Michael J. Turner [a], Mikiyasu Shirai [b], Masaru Sugimachi [a,c]

[a] Department of Cardiovascular Dynamics, National Cerebral and Cardiovascular Center, Osaka 565-8565, Japan
[b] Department of Cardiac Physiology, National Cerebral and Cardiovascular Center, Osaka 565-8565, Japan
[c] Department of Artificial Organ Medicine, Faculty of Medicine, Osaka University Graduate School of Medicine, Osaka 565-0871, Japan

ARTICLE INFO

Article history:
Received 16 July 2014
Received in revised form 6 October 2014
Accepted 15 October 2014

Keywords:
Carotid sinus baroreflex
Open-loop analysis
Arterial pressure
Neuronal uptake blockade

ABSTRACT

Arterial pressure (AP) elevates as a logarithmic function of exogenously administered dose of norepinephrine (NE). In contrast, AP is nearly linearly correlated with efferent sympathetic nerve activity (SNA) during acute baroreflex intervention. The present study aimed at quantifying the relationship between SNA and plasma NE concentration during acute baroreflex intervention. Carotid sinus regions were isolated from systemic circulation in five Wistar Kyoto rats, and carotid sinus pressure was changed among 60, 100, 120, 140, and 180 mm Hg every 2 min. Arterial blood (0.2 ml) was obtained at each pressure level for plasma NE measurement. Maximum AP and minimum AP were 153.34 ± 6.28 and 67.31 ± 4.92 mm Hg, respectively, in response to pressure perturbation. Plasma NE correlated linearly with SNA for individual animal data (slope: 0.957 ± 0.090 $pg \cdot ml^{-1} \cdot \%^{-1}$, intercept: 46.57 ± 7.22 pg/ml, r^2: ranged from 0.923 to 0.992) and also for group averaged data (NE = 0.956 × SNA + 47.97, $r^2 = 0.982$). Blockade of neuronal NE uptake by intravenous desipramine (1 mg/kg) administration increased the slope (2.966 ± 0.686 $pg \cdot ml^{-1} \cdot \%^{-1}$, $P < 0.05$) and the intercept (168.73 ± 28.53 pg/ml, $P < 0.01$) of the plasma NE–SNA relationship. These results indicate that the relationship between SNA and plasma NE concentration was nearly linear within the normal physiological range of acute baroreflex control of AP. While plasma NE concentration can reflect changes in SNA, it may also overestimate the sympathetic outflow from the central nervous system when neuronal NE uptake is impaired systemically.

1. Introduction

The arterial baroreflex is an important negative feedback system that stabilizes arterial pressure (AP) during daily activities. The sympathetic nervous system plays a dominant role in the acute baroreflex control of AP. Studies using an isolated carotid sinus baroreceptor preparation have revealed that AP correlates almost linearly with efferent sympathetic nerve activity (SNA) when examined by a staircase-wise pressure input protocol in anesthetized rats (Kawada et al., 2009, 2010, 2011, 2014; Yamamoto et al., 2013). Norepinephrine (NE) is a neurotransmitter released into the synaptic cleft at sympathetic nerve endings. Although a large portion of NE is removed from the synaptic cleft by neuronal and extraneuronal NE uptake mechanisms (Eisenhofer, 2001; Nicholls, 1994; Shimizu et al., 2010), a fraction of NE is diffused into the bloodstream and can be measured as plasma NE. While it is conceivable that plasma NE concentration reflects the level of SNA, an exact relationship between SNA and plasma NE concentration during an acute baroreflex intervention remains unknown. In contrast to the almost linear AP response to SNA observed in acute baroreflex studies, AP elevates with the logarithm of exogenously administered dose of NE (Yamaguchi and Kopin, 1980) or the logarithm of plasma NE concentration during electrical spinal cord stimulation in pithed rats (Yamaguchi and Kopin, 1979). On the other hand, administration of calcium antagonists exhibits good inverse correlations between AP and the logarithm of plasma NE concentration (Imai et al., 1994). If plasma NE concentration is logarithmically associated with AP, the linearity between SNA and AP would indicate that plasma NE concentration exponentially increases as a function of SNA. To test this hypothesis, the present study aimed to quantify the relationship between SNA and plasma NE concentration during acute baroreflex intervention. In addition, the effect of neuronal NE uptake blockade on the relationship between SNA and plasma NE concentration was explored to quantitatively understand the importance of neuronal NE uptake in the determination of plasma NE concentration.

2. Materials and methods

Animal care was provided in strict accordance with the *Guiding Principles for the Care and Use of Animals in the Field of Physiological*

* Corresponding author at: Department of Cardiovascular Dynamics, National Cerebral and Cardiovascular Center, 5-7-1 Fujishirodai, Suita, Osaka 565-8565, Japan. Tel.:+81 6 6833 5012x2427; fax: +81 6 6835 5403.
E-mail address: torukawa@ncvc.go.jp (T. Kawada).

http://dx.doi.org/10.1016/j.autneu.2014.10.016
1566-0702/

Sciences, approved by the Physiological Society of Japan. All protocols were reviewed and approved by the Animal Subject Committee of National Cerebral and Cardiovascular Center.

Male Wistar Kyoto rats (330–380 g) were anesthetized with an intraperitoneal injection (2 ml/kg) of a mixture of urethane (250 mg/ml) and α-chloralose (40 mg/ml), and mechanically ventilated with oxygen-supplied room air. Anesthesia was maintained by continuous intravenous infusion of a diluted solution of the above anesthetic mixture. An arterial catheter was inserted into the right femoral artery to measure AP. Another arterial catheter was inserted into the left common carotid artery to obtain arterial blood samples. Body temperature of the animal was maintained at approximately 38 °C using a heating pad and a lamp.

A postganglionic branch of the splanchnic sympathetic nerve was exposed retroperitoneally through a left flank incision for the measurement of splanchnic SNA (spSNA). A pair of stainless steel wire electrodes (Bioflex wire, AS633, Cooner Wire, CA, USA) was attached to the nerve, and were secured with silicone glue (Kwik-Sil, World Precision Instruments, FL, USA). A preamplified nerve signal was band-pass filtered at 150 − 1000 Hz, and then full-wave rectified and low-pass filtered at a cut-off frequency of 30 Hz using analog circuits. A ganglionic blocker hexamethonium bromide (60 mg/kg) was given intravenously at the end of the experiment to confirm the disappearance of spSNA and to measure the noise level (Kawada et al., 2010).

The aortic depressor nerves and the vagus nerves were sectioned bilaterally to minimize reflex effects from the aortic arch and cardiopulmonary regions. Bilateral carotid sinuses were isolated from system circulation according to previously reported procedures (Sato et al., 1999; Shoukas et al., 1991). The isolated carotid sinuses were filled with warmed Ringer's solution through catheters inserted into the common carotid arteries. Carotid sinus pressure (CSP) was controlled using a servo-controlled piston pump. Heparin sodium (100 U/kg) was given intravenously to prevent blood coagulation. After completing the above surgery, a stabilization period of at least 60 min was allowed before data acquisition.

2.1. Protocol 1 ($n = 5$)

To determine the time course of plasma NE response to carotid sinus baroreflex, CSP was first set at 100 mm Hg. After AP reached a steady state, CSP was increased to 140 mm Hg. Arterial blood (0.2 ml) was sampled at 80, 50, and 20 s before the step change in CSP and at 30, 60, 90, 120, 150, and 180 s after the step change in CSP. Each blood sampling procedure took approximately 15 s. To avoid contamination of the blood within a catheter, an initial 0.2-ml blood was withdrawn into a temporary syringe that had been filled with 0.2-ml saline, the following 0.2-ml blood was taken as a sample, and then the initial blood, admixed with saline, was returned into the artery. The blood samples were immediately iced to 4 °C. After the end of the protocol, the blood samples were centrifuged and plasma NE concentrations were measured using a high-performance liquid chromatography system (Eicom, Kyoto, Japan) after an alumina adsorption procedure.

2.2. Protocol 2 ($n = 5$)

To determine the relationship between spSNA and plasma NE over a wide input pressure range of the carotid sinus baroreflex, CSP was first decreased to 60 mm Hg for 4 min. CSP was then increased to 100, 120, 140, and 180 mm Hg in a staircase manner. Each step was maintained for 120 s. Based on the time course of plasma NE response obtained in *Protocol 1*, arterial blood (0.2 ml) was sampled at 100 s in each CSP step. The blood sampling procedure took approximately 15 s, as described in *Protocol 1*, and had finished before the next CSP change occurring at 120 s. After obtaining control data, a neuronal uptake blocker desipramine (1 mg/kg) was administered intravenously. Twelve minutes later, the staircase-wise CSP input was repeated and corresponding data were obtained.

2.3. Protocol 3 ($n = 5$)

As a supplemental protocol, the effect of exogenous NE administration on AP was examined. Carotid sinuses were not isolated, and the aortic depressor nerves and vagus nerves were untouched in this group. Instead, ganglionic transmission was blocked by intravenous bolus injection of hexamethonium bromide (60 mg/kg). After 30-min stabilization, the AP response to intravenous continuous administration of NE was examined. The dose of NE was changed every 15 min in an increasing order at 0.05, 0.1, 0.5, 1, 5, 10, 50, 100, 500, and 1000 $\mu g \cdot kg^{-1} \cdot h^{-1}$.

2.4. Data analysis

CSP, spSNA, and AP were recorded at 1000 Hz using a 16-bit analog-to-digital converter. In *Protocol 1*, mean spSNA recorded during CSP of 100 mm Hg was assigned to 100%, and mean spSNA measured after the ganglionic blockade was assigned to 0% in each animal. For plasma NE data, baseline NE concentration was determined from an average of three data points before the step input in each animal. In addition to the absolute NE concentration, the decrease in plasma NE concentration from the baseline value was expressed as a percentage relative to the decrease observed at the nadir (90 s after the step input). In *Protocol 2*, mean spSNA and AP were obtained by averaging spSNA and AP values from 90 to 100 s, just before the arterial blood sampling, at each CSP level. The mean spSNA corresponding to 60-mmHg CSP was assigned to 100%, and mean spSNA measured after the ganglionic blockade was assigned to 0% in each animal. In *Protocol 3*, the AP value corresponding to each NE dose was derived from an average during the last 1 min of the 15-min administration period.

2.5. Statistical analysis

All data are presented as mean and SE values. In *Protocol 1*, plasma NE concentrations at 30, 60, 90, 120, 150, and 180 s after the step input were compared using one-way repeated-measures analysis of variance (ANOVA). In *Protocol 2*, slope and intercept values were determined in each animal by linear regression, and the parameters were compared before and after the desipramine administration using a paired-t test. Differences were considered significant when $P < 0.05$ (Glantz, 2002). In *Protocol 3*, the relationship between exogenously administered dose of NE and AP was examined using a semilog plot (a linear ordinate versus a logarithmic abscissa) and linear scatter plots.

3. Results

Time series of CSP, AP, and spSNA obtained in *Protocol 1*, and corresponding plasma NE concentrations are shown in Fig. 1. CSP and AP are presented as 10-Hz resampled signals, and spSNA is presented as a 2-s moving averaged signal. Before the step increase in CSP, there were transient AP drops caused by arterial blood sampling for the measurement of plasma NE concentration. After CSP was increased, AP showed a sustained reduction. While spSNA was stable before the step input, it ceased at the onset of the step input. Thereafter, spSNA gradually recovered to approximately 35% of the baseline level after 210 s. The baseline plasma NE concentration was approximately 120 pg/ml. After CSP was increased, plasma NE concentration decreased to approximately 80 pg/ml. While there were no statistically significant differences in plasma NE concentration from 30 to 180 s, a slight nadir was observed at 90 s. If decreases from baseline are expressed as percentages relative to the decrease observed at the nadir, percent decreases were 67.1 ± 8.8% at 30 s, 82.9 ± 4.1% at 60 s, and 100% at 90 s. Thereafter, percent

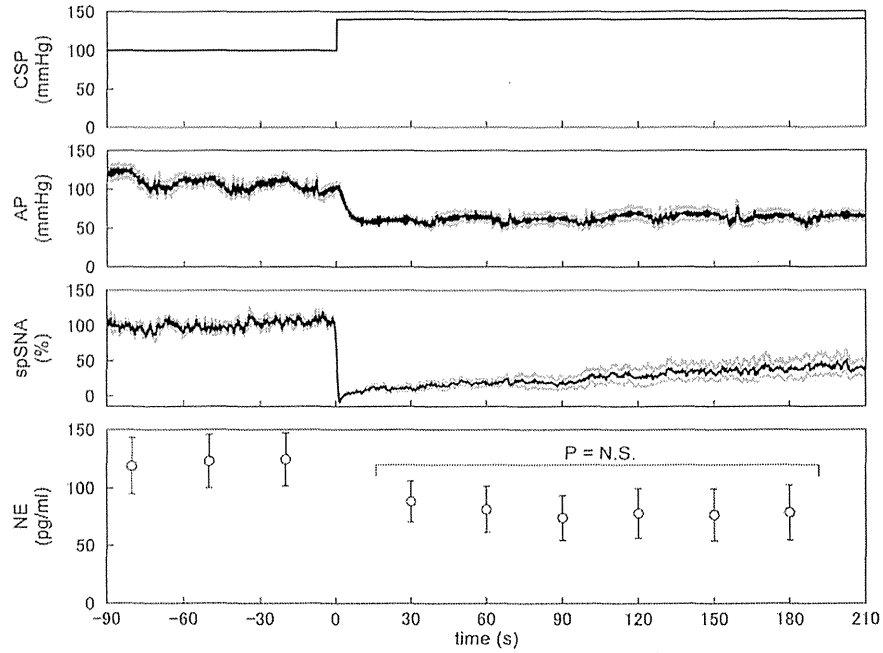

Fig. 1. Time series of carotid sinus pressure (CSP), arterial pressure (AP), and splanchnic sympathetic nerve activity (spSNA), and corresponding plasma norepinephrine (NE) concentration obtained in *Protocol 1*. A step increase in CSP decreased AP and spSNA. Plasma NE concentration decreased in response to the step increase in CSP and did not differ significantly from 30 to 180 s after the step input. Data are mean and SE values.

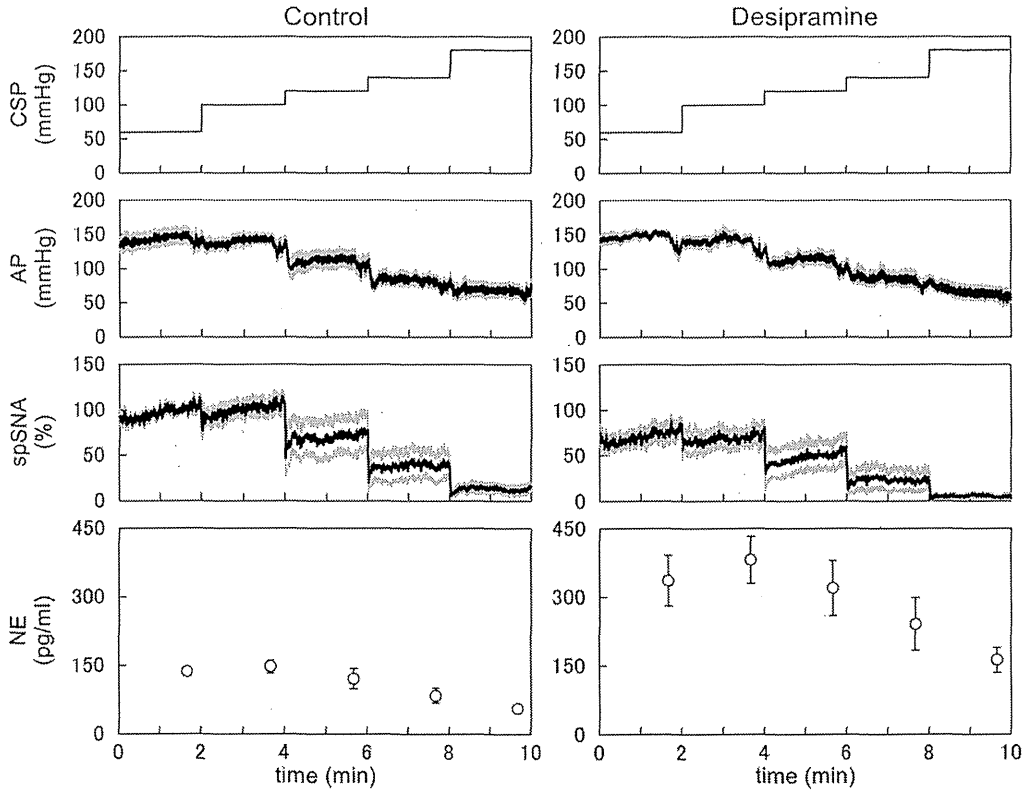

Fig. 2. Time series of arterial pressure (AP) and splanchnic sympathetic nerve activity (spSNA) in response to a staircase-wise increase in carotid sinus pressure (CSP) obtained in *Protocol 2*. Plasma norepinephrine (NE) concentration was decreased as CSP was increased to 120 mm Hg and above. Intravenous administration of desipramine (1 mg/ml) decreased the maximum spSNA but did not change the AP response significantly. Desipramine significantly increased plasma NE concentration compared with the control condition at each corresponding CSP level. Data are mean and SE values.

decreases were relatively stable (92.8 ± 4.5% at 120 s, 93.9 ± 10.8% at 150 s, and 90.4 ± 13.7% at 180 s).

The time series of CSP, AP, and spSNA obtained in *Protocol 2*, and corresponding plasma NE concentrations are shown in Fig. 2. CSP and AP are presented as 10-Hz resampled signals, and spSNA is presented as a 2-s moving averaged signal. An increase in CSP decreased AP and spSNA both under the control condition and after the intravenous administration of desipramine. An increase in CSP from 60 to 100 mm Hg did not decrease plasma NE concentration. Further increases in CSP to 120, 140, and 180 mm Hg decreased plasma NE concentration. Desipramine suppressed the maximum spSNA but did not decrease AP significantly compared with the control condition. Desipramine significantly increased plasma NE concentration compared with the control condition at each CSP level.

In *Protocol 2*, plasma NE concentration was nearly linearly correlated with spSNA for individual animal data with the coefficient of determination (r^2) ranging from 0.923 to 0.992 (Fig. 3A) and also for the group-averaged data with r^2 of 0.982 (Fig. 3G) under the control condition. After desipramine, the data points became convex in two animals (Fig. 3D, "a" and "d") and plasma NE concentrations at high spSNA were greatly dispersed in three animals (Fig. 3D, "b", "d", and "e"). After desipramine, r^2 ranged from 0.791 to 0.940 for individual data (Fig. 3D) and was 0.912 for the group-averaged data (Fig. 3G). On average, desipramine tripled the slope of the regression line (from 0.957 ± 0.090 to 2.966 ± 0.686 pg ml^{-1} $\%^{-1}$, $P < 0.05$) and increased the intercept (from 46.57 ± 7.22 to 168.73 ± 28.53 pg/ml, $P < 0.01$) compared with the control condition (Fig. 3G).

AP was nearly linearly correlated with spSNA for individual animal data with r^2 ranging from 0.855 to 0.991 (Fig. 3B) and also for group-averaged data with r^2 of 0.985 (Fig. 3H) under the control condition. After desipramine, AP was nearly linearly correlated with spSNA for individual data with r^2 ranging from 0.892 to 0.975 (Fig. 3E) and also for group-averaged data with r^2 of 0.997 (Fig. 3H). Desipramine increased the slope of AP versus spSNA (from 0.878 ± 0.082 to 1.212 ± 0.100 mm Hg/%, $P < 0.01$) but did not change the intercept (from 54.16 ± 7.64 to 59.64 ± 6.18%, $P = 0.37$) compared with the control condition (Fig. 3H).

The minimum spSNA was 11.36 ± 4.37% and the maximum spSNA was 106.94 ± 6.02% under the control condition. Note that the maximum spSNA occurred at the CSP level higher than 60 mm Hg in two

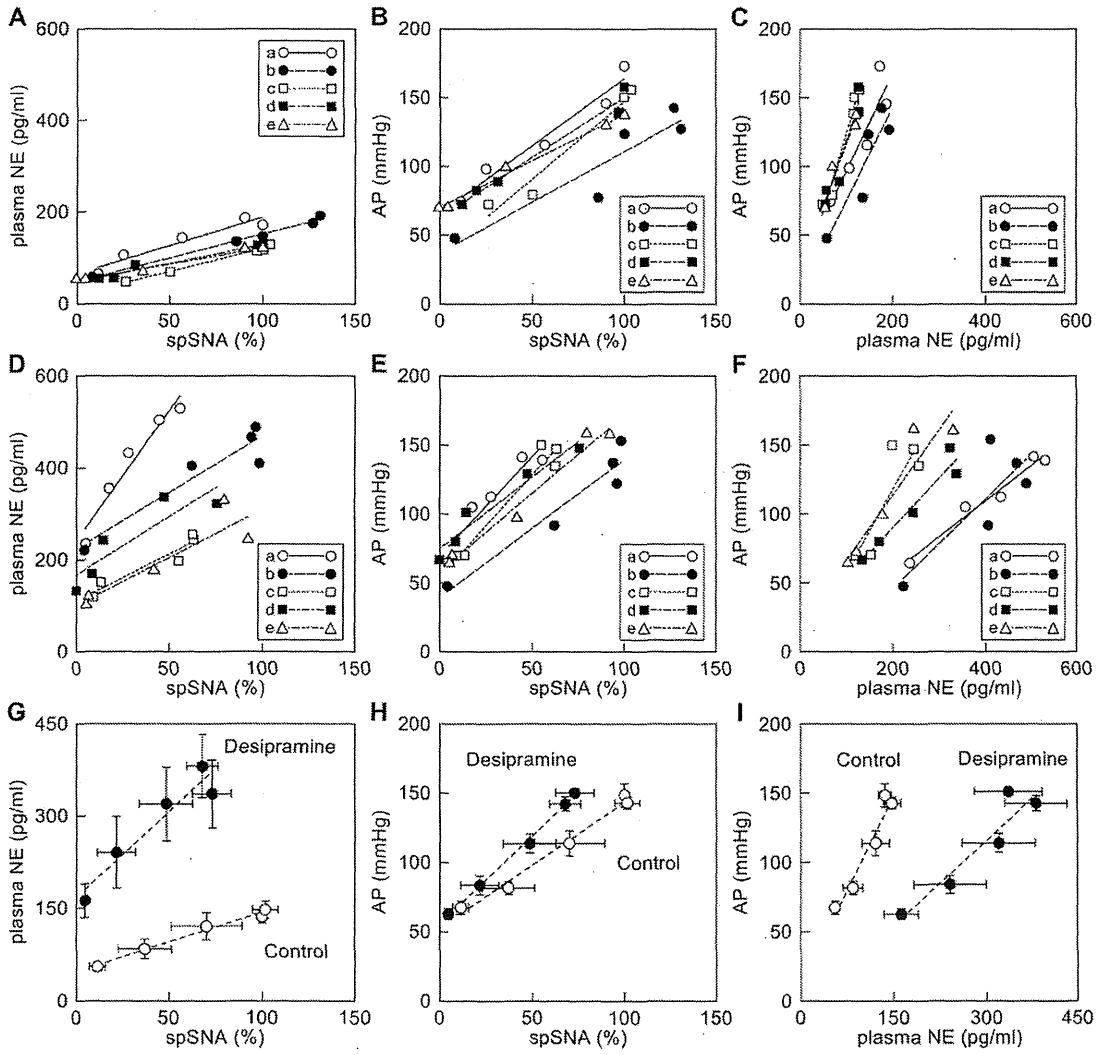

Fig. 3. Relationships between splanchnic sympathetic nerve activity (spSNA) and plasma norepinephrine (NE) concentration (A), spSNA and arterial pressure (AP) (B), and plasma NE concentration and AP (C) under the control condition. Relationships between spSNA and plasma NE concentration (D), spSNA and AP (E), and plasma NE concentration and AP (F) after the intravenous administration of desipramine. In panels A–F, different symbols and regression lines indicate data from different animals. Group-averaged relationships between spSNA and plasma NE concentration (G), spSNA and AP (H), and plasma NE concentration and AP (I) before (open circles) and after (filled circles) intravenous administration of desipramine. In panels G, H, and I, data points indicate mean and SE values, and dotted lines are linear regression lines on averaged data points.

animals, and hence exceeded 100%. Desipramine did not affect the minimum spSNA (4.58 ± 1.50%, P = 0.16) but decreased the maximum spSNA (77.00 ± 8.16%, P = 0.01) compared with the control condition. The minimum AP was 67.31 ± 4.92 mm Hg, the maximum AP was 153.34 ± 6.28 mm Hg, and the range of AP response (i.e., the maximum AP minus the minimum AP) was 86.04 ± 5.43 mm Hg under the control condition. Desipramine decreased the minimum AP (62.74 ± 3.86 mm Hg, P < 0.05) but did not affect the maximum AP (151.16 ± 3.29 mm Hg, P = 0.83) or the range of AP response (88.42 ± 5.67 mm Hg, P = 0.80) compared with the control condition.

AP was nearly linearly correlated with plasma NE concentration for individual animal data with r^2 ranging from 0.817 to 0.965 (Fig. 3C) and also for group-averaged data with r^2 of 0.943 (Fig. 3I) under the control condition. Data points at high AP were greatly dispersed after desipramine, resulting in r^2 ranging from 0.661 to 0.968 for individual data (Fig. 3F) and 0.889 for group-averaged data (Fig. 3I). Desipramine halved the slope of the regression line (from 0.896 ± 0.085 to 0.403 ± 0.061 mm Hg·pg^{-1}·ml, P < 0.001) and tended to decrease the intercept (16.47 ± 3.76 to 4.71 ± 7.03 mm Hg, P = 0.066) compared with the control condition (Fig. 3I).

In *Protocol 3*, AP was linearly correlated with the logarithm of the exogenously administered dose of NE (Fig. 4A). The solid line represents linear regression of AP versus the logarithm of the dose of NE. When linear scales were used, the relationship between the dose of NE and AP did not approximate a straight line even when the range of exogenous NE was limited up to 10 (Fig. 4B) or 100 μg·kg^{-1}·h^{-1} (Fig. 4C). In Fig. 4B and C, the solid curve represents the regression, AP = a × $\log_{10}$(NE) + b, determined from the data points up to 1000 μg·kg^{-1}·h^{-1} of NE. The dotted curve also represents the regression but determined from the data points up to 10 (Fig. 4B) or 100 μg·kg^{-1}·h^{-1} (Fig. 4C) of NE. In Fig. 4B and C, the baseline AP after ganglionic blockade was depicted as a filled circle at NE = 0.

4. Discussion

4.1. Relationship between spSNA and plasma NE concentration

As mentioned in the Introduction section, AP changes almost linearly with the amplitude of multifiber spSNA during acute baroreflex intervention (Fig. 3H). In contrast, AP increases with the logarithm of exogenously administered dose of NE (Fig. 4A), and plots of AP versus the dose of NE cannot be linear even when the NE range was limited to lower doses (Fig. 4B and C). Yamaguchi and Kopin (1979) demonstrated that AP increases as a function of the logarithm of plasma NE concentration during electrical spinal cord stimulation in pithed rats. While these results suggest a possible exponential increase of plasma NE concentration as a function of SNA, the present results demonstrated nearly linear relationship between spSNA and plasma NE concentration during acute baroreflex intervention under the control condition (Fig. 3G). The relationship between plasma NE concentration and AP was also almost linear under the control condition (Fig. 3I). Although the maximum sympathetic activation attained by baroreceptor unloading alone might be lower than that attained by direct electrical stimulation of the spinal cord (Yamaguchi and Kopin, 1979), the maximum AP reached 150 mm Hg in *Protocol 2* (Fig. 3I). Therefore, it is likely that the relationship between plasma NE concentration and AP is more linear than commonly thought when examined within the physiological range of baroreflex-mediated AP control. On the other hand, when renal SNA is enhanced by passive muscle stretch on top of the baroreceptor unloading, the AP response becomes saturated, rendering the AP–renal SNA relationship convex curvilinear (Yamamoto et al., 2005). If such data points of excess sympathetic activation are included, AP may be more linearly correlated with the logarithm of SNA and hence the logarithm of plasma NE concentration.

Plasma NE concentrations measured under the control condition (Fig. 3) were lower than those observed during electrical spinal cord stimulation in pithed rats in the absence of anesthesia when compared at the same degree of AP elevation (Yamaguchi and Kopin, 1979). While the maximum AP seemed maintained, anesthesia might have suppressed a sympathetic tone and reduced plasma NE concentration in the present study. Another possible explanation is that the leakage of NE from the sympathetic nerve terminals into the circulation might have been smaller during the baroreflex-mediated sympathetic intervention compared with the sympathetic activation by spinal cord stimulation. Coordinated sympathetic activation among different neural districts is important for the AP control (Guyenet, 2006). While the pithed preparation is useful for investigating sympathetic cardiovascular regulations (Yamaguchi and Kopin, 1979, 1980), stimulation from the spinal cord eliminates the coordinated sympathetic activation. In contrast, because the baroreflex-mediated sympathetic intervention maintains the integrity of the sympathetic pathway from the vasomotor center to the effector organs, the sympathetic nervous system might have operated more efficiently to increase AP. While the stimulation patterns alone (constant, irregular, or burst) do not affect NE overflow or vasoconstriction significantly (Kahan et al., 1988), intermittent and irregular bursting diamond-wave pattern is more effective in reproducing renal functional alterations than continuous square wave pattern (DiBona and Sawin, 1999). Further studies are clearly required to compare the effectiveness of native sympathetic discharge versus electrical stimulation-induced sympathetic activation in the control of AP.

Despite a significant advancement of SNA recording technique in rats (Stocker and Muntzel, 2013), the quantification of chronic changes

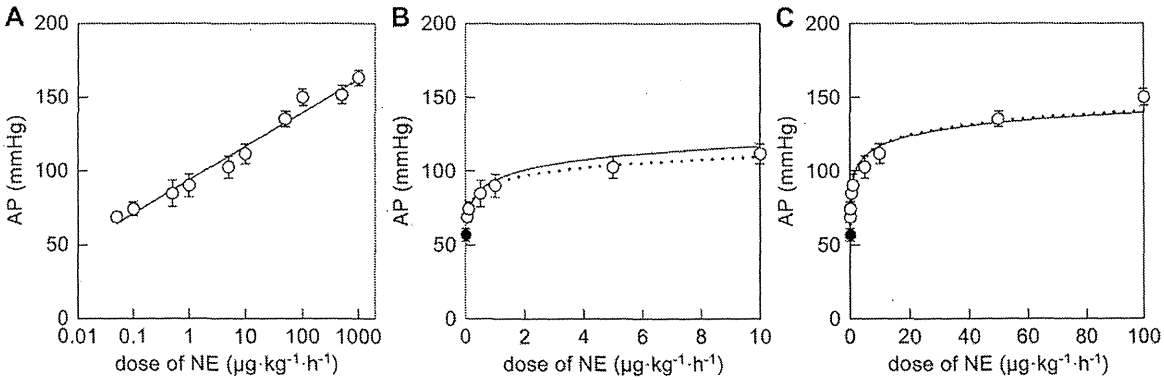

Fig. 4. Relationship between exogenously administered dose of norepinephrine (NE) and steady-state arterial pressure (AP) response shown as a semilog plot (a linear ordinate versus a logarithmic abscissa) (A) and linear scaled scatter plots (B and C). The linear plots include the baseline AP after the ganglionic blockade at NE = 0. The solid line in panel A indicates a linear regression line for AP versus the logarithm of NE. The solid curves in panels B and C indicate the regression, AP = a × $\log_{10}$(NE) + b, determined using all data points up to 1000 μg kg^{-1} h^{-1} of NE. The dotted curve indicates the same regression but determined using data points up to 10 (B) and 100 (C) μg kg^{-1} h^{-1} of NE. Data are mean and SE values.

in SNA over long periods (e.g., weeks) is still challenging due to potential time-dependent decline in the amplitude of SNA. The present study demonstrated a nearly linear relationship between plasma NE and spSNA during acute baroreflex intervention (Fig. 3G). If such relationship between SNA and plasma NE is consistent over longer periods, plasma NE levels could be used as a surrogate for SNA. To determine whether plasma NE levels can be a surrogate for SNA in chronic experimental settings may be one of the future directions of the study.

4.2. Effects of neuronal uptake blockade on spSNA and plasma NE concentration

In *Protocol 2*, maximum spSNA was reduced after the desipramine administration, which is consistent with previous reports observed in renal SNA (Eisenhofer et al., 1991) and cardiac SNA (Kawada et al., 2004) in rabbits. Neuronal NE uptake blockade by desipramine results in the accumulation of synaptic NE of the noradrenergic neurons in the central nervous system, which would cause presynaptic inhibition via α_2-adrenegic receptors (Svensson and Usdin, 1978). On the other hand, the accumulation of synaptic NE at the neuroeffector junction can enhance the peripheral cardiovascular response, as evidenced by the increased slope of the AP response to spSNA (Fig. 3H). The results are in agreement with enhanced NE release and AP response to spinal cord stimulation by desipramine (Yamaguchi and Kopin, 1980). Because of the enhanced peripheral cardiovascular response, maximum AP after desipramine was not much different compared with the control condition despite the lower maximum spSNA in *Protocol 2*. The enhanced peripheral cardiovascular response is, however, somewhat divergent from the effects of desipramine on dynamic baroreflex regulation, because the transfer function from cardiac SNA to AP was unchanged by desipramine (Kawada et al., 2004). While desipramine-induced accumulation of synaptic NE contributes to the maintenance of mean AP, it can reduce the relative change of synaptic NE concentration per nerve impulse, resulting in the limited dynamic AP response. As another example, desipramine decreases the dynamic gain of the hind-limb vascular conductance response to electrical stimulation of the lumber sympathetic chain (Bertram et al., 2000). These results indicate that dynamic response and steady-state response need to be separately assessed when evaluating the effects of neuronal NE uptake blockade on peripheral cardiovascular responses.

Impairment of neuronal NE uptake may contribute to the pathophysiology of sympathetic abnormality in heart failure (Backs et al., 2001) and hypertension (Rumantir et al., 2000). Cardiac overexpression of NE transporter results in functional improvement of a rabbit model of rapid pacing-induced heart failure (Münch et al., 2005). In the present study, the plasma NE concentration was significantly increased after desipramine compared with the control condition, being consistent with previous reports (Eisenhofer, 2001; Eisenhofer et al., 1991). The increase in plasma NE concentration, in conjunction with the decrease in spSNA, tripled the slope of the regression line between spSNA and plasma NE concentration (Fig. 3G). These results indicate that plasma NE concentration can be increased disproportionally to spSNA depending on the impairment of neuronal NE uptake function. While plasma NE concentration can be an index of spSNA, it could overestimate sympathetic outflow from the central nervous system under diseased conditions when they are associated with the systemic impairment of neuronal NE uptake function.

4.3. Limitations

First, data were obtained under anesthetized conditions. Because anesthesia affects the autonomic nervous activities, the present results may not be directly extrapolated to interpret sympathetic AP control under conscious conditions. Second, time resolution for plasma NE measurement was 30 s, which was by far slower than the recording of spSNA and AP. The necessity of a blood sample volume of 0.2 ml also limited the number of data points analyzed during baroreflex response compared with previous baroreflex studies (Kawada et al., 2009, 2010; Yamamoto et al., 2013). Further refinement of NE measurement to reduce sample volume and increase time resolution will be required to understand dynamic changes in plasma NE concentration during acute baroreflex control of AP.

5. Conclusion

While the logarithmic relation between plasma NE concentration and AP is commonly observed in several circumstances (Imai et al., 1994; Yamaguchi and Kopin, 1979), the relationship between spSNA and plasma NE concentration was nearly linear within the normal physiological range of the acute baroreflex control of AP. Although plasma NE concentration can be an index of spSNA, data needs to be carefully interpreted as the systemic impairment of neuronal NE uptake can increase plasma NE concentration disproportionally to sympathetic outflow from the central nervous system.

Conflict of interest statement

The authors declare that there are no conflicts of interest.

Acknowledgments

This study was supported by the Support Program to break the bottlenecks at R&D System for accelerating the practical use of Health Research Outcome from Japan Science and Technology Agency, and by the Grant-in-Aid for Scientific Research (JSPS KAKENHI Grant Number 26750153).

References

Backs, J., Haunstetter, A., Gerber, S.H., Metz, J., Borst, M.M., Strasser, R.H., Kübler, W., Haass, M., 2001. The neuronal norepinephrine transporter in experimental heart failure: evidence for a posttranscriptional downregulation. J. Mol. Cell. Cardiol. 33, 461–472.
Bertram, D., Barrés, C., Cheng, Y., Julien, C., 2000. Norepinephrine reuptake, baroreflex dynamics, and arterial pressure variability in rats. Am. J. Physiol. Regul. Integr. Comp. Physiol. 279, R1257–R1267.
DiBona, G.F., Sawin, L.L., 1999. Functional significance of the pattern of renal sympathetic nerve activation. Am. J. Physiol. 277, R346–R353.
Eisenhofer, G., 2001. The role of neuronal and extraneuronal plasma membrane transporters in the inactivation of peripheral catecholamines. Pharmacol. Ther. 91, 35–62.
Eisenhofer, G., Saigusa, T., Esler, M.D., Cox, H.S., Angus, J.A., Dorward, P.K., 1991. Central sympathoinhibition and peripheral neuronal uptake blockade after desipramine in rabbits. Am. J. Physiol. 260, R824–R832.
Glantz, S.A., 2002. Primer of Biostatistics, 5th ed. McGraw-Hill, New York.
Guyenet, P.G., 2006. The sympathetic control of blood pressure. Nat. Rev. Neurosci. 7, 335–346.
Imai, K., Higashidate, S., Prados, P.P., Santa, T., Adachi-Akahane, S., Nagao, T., 1994. Relation between blood pressure and plasma catecholamine concentration after administration of calcium antagonists to rats. Biol. Pharm. Bull. 17, 907–910.
Kahan, T., Pernow, J., Schwieler, J., Wallin, B.G., Lundberg, J.M., Hjemdahl, P., 1988. Noradrenaline release evoked by a physiological irregular sympathetic discharge pattern is modulated by prejunctional α- and β-adrenoceptors in vivo. Br. J. Pharmacol. 95, 1101–1108.
Kawada, T., Miyamoto, T., Uemura, K., Kashihara, K., Kamiya, A., Sugimachi, M., Sunagawa, K., 2004. Effects of neuronal norepinephrine uptake blockade on baroreflex neural and peripheral arc transfer characteristics. Am. J. Physiol. Regul. Integr. Comp. Physiol. 286, R1110–R1120.
Kawada, T., Kamiya, A., Li, M., Shimizu, S., Uemura, K., Yamamoto, H., Sugimachi, M., 2009. High levels of circulating angiotensin II shift the open-loop baroreflex control of splanchnic sympathetic nerve activity, heart rate and arterial pressure in anesthetized rats. J. Physiol. Sci. 59, 447–455.
Kawada, T., Li, M., Kamiya, A., Shimizu, S., Uemura, K., Yamamoto, H., Sugimachi, M., 2010. Open-loop dynamic and static characteristics of the carotid sinus baroreflex in rats with chronic heart failure after myocardial infarction. J. Physiol. Sci. 60, 283–298.
Kawada, T., Shimizu, S., Li, M., Kamiya, A., Uemura, K., Sata, Y., Yamamoto, H., Sugimachi, M., 2011. Contrasting effects of moderate vagal stimulation on heart rate and carotid sinus baroreflex-mediated sympathetic arterial pressure regulation in rats. Life Sci. 89, 498–503.
Kawada, T., Li, M., Zheng, C., Shimizu, S., Uemura, K., Turner, M.J., Yamamoto, H., Sugimachi, M., 2014. Chronic vagal nerve stimulation improves baroreflex neural arc function in heart failure rats. J. Appl. Physiol. 116, 1308–1314.

Münch, G., Rosport, K., Bültmann, A., Baumgartner, C., Li, Z., Laacke, L., Ungerer, M., 2005. Cardiac overexpression of the norepinephrine transporter uptake-1 results in marked improvement of heart failure. Circ. Res. 97, 928–936.
Nicholls, D.G., 1994. Proteins, Transmitters and Synapses. Blackwell Sciences, Oxford, UK, pp. 200–221.
Rumantir, M.S., Kaye, D.M., Jennings, G.L., Vaz, M., Hastings, J.A., Esler, M.D., 2000. Phenotypic evidence of faulty neuronal norepinephrine reuptake in essential hypertension. Hypertension 36, 824–829.
Sato, T., Kawada, T., Miyano, H., Shishido, T., Inagaki, M., Yoshimura, R., Tatewaki, T., Sugimachi, M., Alexander Jr., J., Sunagawa, K., 1999. New simple methods for isolating baroreceptor regions of carotid sinus and aortic depressor nerves in rats. Am. J. Physiol. 276, H326–H332.
Shimizu, S., Akiyama, T., Kawada, T., Shishido, T., Mizuno, M., Kamiya, A., Yamazaki, T., Sano, S., Sugimachi, M., 2010. In vivo direct monitoring of interstitial norepinephrine levels at the sinoatrial node. Auton. Neurosci. 152, 115–118.
Shoukas, A.A., Callahan, C.A., Lash, J.M., Haase, E.B., 1991. New technique to completely isolate carotid sinus baroreceptor regions in rats. Am. J. Physiol. 260, H300–H303.
Stocker, S.D., Muntzel, M.S., 2013. Recording sympathetic nerve activity chronically in rats: surgery techniques, assessment of nerve activity, and quantification. Am. J. Physiol. Heart Circ. Physiol. 305, H1407–H1416.
Svensson, T.H., Usdin, T., 1978. Feedback inhibition of brain noradrenaline neurons by tricyclic antidepressants: α-receptor mediation. Science 202, 1089–1091.
Yamaguchi, I., Kopin, I.J., 1979. Plasma catecholamine and blood pressure responses to sympathetic stimulation in pithed rats. Am. J. Physiol. 237, H305–H310.
Yamaguchi, I., Kopin, I.J., 1980. Blood pressure, plasma catecholamines, and sympathetic outflow in pithed SHR and WKY rats. Am. J. Physiol. 238, H365–H372.
Yamamoto, K., Kawada, T., Kamiya, A., Takaki, H., Sugimachi, M., Sunagawa, K., 2005. Static interaction between muscle mechanoreflex and arterial baroreflex in determining efferent sympathetic nerve activity. Am. J. Physiol. Heart Circ. Physiol. 289, H1604–H1609.
Yamamoto, H., Kawada, T., Shimizu, S., Kamiya, A., Miyazaki, S., Sugimachi, M., 2013. Effects of cilnidipine on sympathetic outflow and sympathetic arterial pressure and heart rate regulations in rats. Life Sci. 92, 1202–1207.

Circulation Journal
Official Journal of the Japanese Circulation Society
http://www.j-circ.or.jp

ORIGINAL ARTICLE
Arrhythmia/Electrophysiology

Electrocardiographic Predictors of Response to Cardiac Resynchronization Therapy in Patients With Intraventricular Conduction Delay

Yoichi Takaya, MD; Takashi Noda, MD, PhD; Ikutaro Nakajima, MD; Yuko Yamada, MD; Koji Miyamoto, MD; Hideo Okamura, MD; Kazuhiro Satomi, MD, PhD; Takeshi Aiba, MD, PhD; Kengo F. Kusano, MD, PhD; Hideaki Kanzaki, MD; Toshihisa Anzai, MD, PhD; Masaharu Ishihara, MD, PhD; Satoshi Yasuda, MD, PhD; Hisao Ogawa, MD, PhD; Shiro Kamakura, MD, PhD; Wataru Shimizu, MD, PhD

Background: Little is known about predictors of response to cardiac resynchronization therapy (CRT) in patients with intraventricular conduction delay (IVCD). The purpose of this study was to investigate the benefits of CRT and significant variables on surface electrocardiogram (ECG) to predict response to CRT in those patients.

Methods and Results: Among the cohort of 152 CRT patients, 40 patients with IVCD were evaluated. Sixteen patients (40%) were responders. At baseline, responders had a wider QRS duration (158±18 vs. 144±18 ms, P=0.02) and a higher frequency of left axis deviation (LADEV; 75% vs. 29%, P=0.004) compared with non-responders. After CRT, greater shortening of QRS duration (ΔQRS; 26±24 vs. 7±24 ms, P=0.02), axis shift from LADEV to right axis deviation (RADEV; 69% vs. 13%, P<0.001), and both rightward forces in lead I and anterior forces in V1 (56% vs. 13%, P=0.003) were found more frequently in responders. Multivariable logistic regression analysis showed that LADEV at baseline, or ΔQRS and axis shift from LADEV to RADEV after CRT were independent predictors of response to CRT.

Conclusions: Patients with IVCD may not respond to CRT, but LADEV at baseline and reversal of ventricular activation after CRT on surface ECG could be important to predict response to CRT. (*Circ J* 2014; **78:** 71–77)

Key Words: Cardiac resynchronization therapy; Electrocardiogram; Heart failure; Intraventricular conduction delay; Responder

Cardiac resynchronization therapy (CRT) has improved quality of life, exercise capacity, left ventricular (LV) function, and mortality risk for heart failure due to severe LV systolic dysfunction with prolonged QRS duration.[1–6] The large majority of patients enrolled in CRT trials have had a left bundle branch block (LBBB). Thus, the benefits of CRT in patients with other QRS morphologies, especially non-specific intraventricular conduction delay (IVCD), have not been clearly demonstrated, and little is known about predictors of response to CRT in those patients.

In the presence of LBBB, the right ventricle is activated first followed by right-to-left trans-septal myocardial activation of the left ventricle. This results in late activation of the LV lateral wall. The concept of CRT is to minimize LV conduction delay, which reduces contractile asynchrony and improves LV mechanics by coordinating contraction of the interventricular septum and lateral left ventricle.[7] The resynchronization of electromechanical activation induces LV volume reduction and increased LV ejection fraction (LVEF).[8,9] Therefore, patients with left-sided electrical LV conduction delay are likely to benefit from CRT. In addition, a recent study suggested that LV conduction delay and reversal of ventricular activation after CRT (eg, left→right, posterior→anterior activation reversal) anticipated the likelihood of response to CRT in patients with LBBB.[10]

Accordingly, we hypothesized that left-sided electrical LV conduction delay at baseline and changes in ventricular activation after CRT might be useful to identify appropriate candidates for CRT in patients with IVCD. The purpose of this study was to investigate the benefits of CRT and significant variables on

Received December 20, 2012; revised manuscript received August 15, 2013; accepted September 17, 2013; released online October 25, 2013 Time for primary review: 26 days

Divisions of Arrhythmia and Electrophysiology (Y.T., T.N., I.N., Y.Y., K.M., H. Okamura, K.S., T. Aiba, K.F.K., S.K., W.S.), Heart Failure (H.K., T. Anzai), Department of Cardiovascular Medicine (M.I., S.Y., H. Ogawa), National Cerebral and Cardiovascular Center, Suita; Department of Cardiovascular Medicine, Graduate School of Medical Sciences, Kumamoto University, Kumamoto (H. Ogawa); and Department of Cardiovascular Medicine, Nippon Medical School, Tokyo (W.S.), Japan

Mailing address: Takashi Noda, MD, PhD, Division of Arrhythmia and Electrophysiology, National Cerebral and Cardiovascular Center, 5-7-1 Fujishiro-dai, Suita 565-8565, Japan. E-mail: tnoda@hsp.ncvc.go.jp

ISSN-1346-9843 doi:10.1253/circj.CJ-12-1569

Table 1. Clinical Characteristics

	Responders (n=16)	Non-responders (n=24)	P-value
Age (years)	63±8	58±16	0.24
Male	11 (69)	19 (79)	0.47
Etiology of heart failure			
Ischemic heart disease	3 (19)	7 (29)	0.47
Non-ischemic heart disease	13 (81)	17 (71)	
Medication			
β-blockers	13 (81)	20 (83)	0.87
ACEIs or ARBs	15 (94)	18 (75)	0.13
Duiretics	15 (94)	22 (92)	0.81
Amiodarone	9 (56)	11 (46)	0.53
Atrial fibrillation	3 (19)	3 (13)	0.60
NYHA functional class	3.0±0.5	3.2±0.6	0.35
LV ejection fraction (%)	23±10	28±9	0.07
LV end-systolic volume (ml)	189±88	161±66	0.26
LV end-diastolic volume (ml)	251±103	236±78	0.60
Mitral regurgitation	1.6±1.1	1.7±0.8	0.87
Dyssynchrony	9 (56)	12 (50)	0.71
LV-RV delay (ms)	45±19	47±35	0.88
LV pacing site			
lateral/posterior/anterolateral	12 (75)/3 (19)/1 (6)	15 (63)/7 (29)/2 (8)	0.47
RV pacing site			
apex/septum	15 (94)/1 (6)	22 (92)/2 (8)	0.81
After CRT			
NYHA functional class	1.5±0.5	1.9±0.7	0.04
LV ejection fraction (%)	29±13	27±10	0.76
LV end-systolic volume (ml)	147±68	164±77	0.47
LV end-diastolic volume (ml)	199±70	226±87	0.31
Mitral regurgitation	1.4±1.0	1.3±0.9	0.87
Change in LV ejection fraction (%)	7±5	−2±5	<0.001
Change in LV end-systolic volume (ml)	−42±23	4±31	<0.001
Change in LV end-diastolic volume (ml)	−52±103	−9±33	0.003
Change in mitral regurgitation	−0.2±0.5	−0.3±0.8	0.59

Data given as mean±SD or n (%).
ACEI, angiotensin-converting enzyme inhibitor; ARB, angiotensin receptor blocker; CRT, cardiac resynchronization therapy; LV, left ventricular; NYHA, New York Heart Association; RV, right ventricular.

the surface electrocardiogram (ECG) to predict the response to CRT in those patients.

Methods

Subjects

Among the cohort of 152 consecutive patients who had CRT device implanted at the National Cardiovascular and Cardiovascular Center in Suita, Japan, from January 2005 to April 2010, 40 patients with IVCD on baseline ECG were enrolled in this study. The indications for CRT were heart failure symptoms despite optimal medication; New York Heart Association (NYHA) functional class II–IV; LVEF ≤35%; and QRS duration ≥120 ms. IVCD was defined as QRS duration ≥120 ms without typical LBBB (QS or rS in V1 and broad R waves without Q waves in lead I or V6) or typical right BBB (qR or rSR in V1 and deep S waves in lead I and V6). This study was approved by the institutional ethics committee, and written informed consent was obtained from all patients.

ECG Assessment

Surface 12-lead ECGs were acquired at a paper speed of 25 mm/s and a scale of 10 mm/mV at baseline and immediately after CRT device implantation. Assessments of QRS duration, QRS axis, and QRS patterns were performed by 2 independent cardiologists who were blinded to other data of the patients. QRS duration was measured from its first deflection to its end. Normal frontal plane axis was +90° to <−30°, left axis deviation (LADEV) was ≥−30° to −90°, and right axis deviation (RADEV) was >+90° to 180°. QRS patterns in each lead were classified into R, RS (R=S and both >1 mm, or both <1 mm), Rs (R>s), rS (r<S), QS, qR (q<R), QR (Q=R and both >1 mm, or both <1 mm), Qr (Q>r), and QRS (all 3 waveforms present). We analyzed these ECG findings at baseline and immediately after CRT device implantation.

Echocardiographic Assessment

All patients underwent complete echocardiography at baseline and at 6 months after CRT device implantation. Complete M-mode, 2-D, and Doppler evaluations were performed. Images were obtained using a 3.5-MHz transducer at an appropriate depth in the parasternal and apical views. LV end-systolic volume, LV end-diastolic volume, and LVEF were calculated using the biplane Simpson's technique. Mitral regurgitation was grad-